

1            Geometric models reveal behavioral and neural  
2            signatures of how naturalistic experiences are  
3            transformed into episodic memories

4            Andrew C. Heusser<sup>1, 2, †</sup>, Paxton C. Fitzpatrick<sup>1, †</sup>, and Jeremy R. Manning<sup>1, \*</sup>

<sup>1</sup>Department of Psychological and Brain Sciences

Dartmouth College, Hanover, NH 03755, USA

<sup>2</sup>Akili Interactive

Boston, MA 02110

<sup>†</sup>Denotes equal contribution

<sup>\*</sup>Corresponding author: Jeremy.R.Manning@Dartmouth.edu

5            August 20, 2020

6            **Abstract**

7            Our ongoing subjective experience reflects external sensory information from each moment,  
8            along with additional information from our past that we carry with us into that moment. The  
9            blend of memories, knowledge, emotions, goals, and other internal perceptual and mental states  
10          that color our subjective experience provides a *context* for interpreting new information and  
11          conceptually linking what is happening now with our prior experiences. Because this contextual  
12          information is often person-specific, the subjective experience that each person encodes into their  
13          memory is often idiosyncratic, even for shared experiences and sensory perspectives. We sought  
14          to study which aspects of a shared naturalistic experience were preserved or distorted, and how  
15          those distortions compared across individuals. To this end, we developed a geometric frame-

16 work for mathematically characterizing the subjective conceptual content of dynamic naturalistic  
17 experiences. We model experiences as *trajectories* through word embedding spaces whose coor-  
18 dinates reflect the universe of thoughts under consideration. We also demonstrate how *memories*  
19 may also be modeled as trajectories through the same spaces. According to this view, encod-  
20 ing an experience into memory entails geometrically distorting or transforming the *shape* of the  
21 original experience’s trajectory. This translates qualitative, neuropsychological questions about  
22 how we remember naturalistic experiences into quantitative, geometric questions about the spatial  
23 configurations of trajectory shapes. We applied our framework to data collected as participants  
24 watched and verbally recounted a television episode while undergoing functional neuroimaging.  
25 We found that the trajectories of participants’ recounts of the episode nearly all captured  
26 the coarse spatial properties of the original episode’s trajectory (i.e., the essential plot points),  
27 but participants differed in their memory for fine details. We also identified a network of brain  
28 structures that were sensitive to the shape of the episode’s trajectory through word embedding  
29 space, and an overlapping network that predicted, at the time of encoding, how people would  
30 distort (transform) the episode’s trajectory when they recounted the episode later. Our work  
31 provides insights into how our brains distort and transform our ongoing experiences when we  
32 encode them into episodic memories.

## 33 **Introduction**

34 What does it mean to *remember* something? In traditional episodic memory experiments (e.g.,  
35 list-learning or trial-based experiments; Murdock, 1962; Kahana, 1996), remembering is often cast  
36 as a discrete and binary operation: each studied item may be separated from the rest of one’s  
37 experience and singularly labeled as having been recalled or forgotten. More nuanced studies  
38 might incorporate self-reported confidence measures as a proxy for memory strength, or ask  
39 participants to discriminate between “recollecting” the (contextual) details of an experience or  
40 having a general feeling of “familiarity” (Yonelinas, 2002). Using well-controlled, trial-based  
41 experimental designs, the field has amassed a wealth of information regarding human episodic  
42 memory. However, there are fundamental properties of the external world and our memories that

43 trial-based experiments are not well suited to capture (for review, also see Koriat and Goldsmith,  
44 1994; Huk et al., 2018). First, our experiences and memories are continuous, rather than discrete—  
45 isolating a (naturalistic) event from the context in which it occurs can substantially change its  
46 meaning. Second, whether or not the rememberer has precisely reproduced a specific set of words  
47 in describing a given experience is nearly orthogonal to how well they were actually able to  
48 remember it. In classic (e.g., list-learning) memory studies, by contrast, the number or proportion  
49 of *exact* recalls is often considered to be a primary metric for assessing the quality of participants'  
50 memories. Third, one might remember the *essence* (or a general summary) of an experience but  
51 forget (or neglect to recount) particular details. Capturing the essence of what happened is often  
52 a main goal of recounting an episodic memory to a listener, whereas the inclusion of specific,  
53 low-level details is often less pertinent.

54 How might we formally characterize the *essence* of an experience, and whether it has been  
55 recovered by the rememberer? And how might we distinguish an experience's overarching essence  
56 from its low-level details? One approach is to start by considering some fundamental properties  
57 of the dynamics of our experiences. Each given moment of an experience tends to derive meaning  
58 from surrounding moments, as well as from longer-range temporal associations (Lerner et al., 2011;  
59 Manning, 2019, 2020). Therefore, the timecourse describing how an event unfolds is fundamental  
60 to its overall meaning. Further, this hierarchy formed by our subjective experiences at different  
61 timescales defines a *context* for each new moment (e.g., Howard and Kahana, 2002; Howard  
62 et al., 2014), and plays an important role in how we interpret that moment and remember it  
63 later (for review see Manning et al., 2015; Manning, 2020). Our memory systems can leverage  
64 these associations to form predictions that help guide our behaviors (Ranganath and Ritchey,  
65 2012). For example, as we navigate the world, the features of our subjective experiences tend  
66 to change gradually (e.g., the room or situation we find ourselves in at any given moment is  
67 strongly temporally autocorrelated), allowing us to form stable estimates of our current situation  
68 and behave accordingly (Zacks et al., 2007; Zwaan and Radvansky, 1998).

69 Occasionally, this gradual “drift” of our ongoing experience is punctuated by sudden changes,  
70 or “shifts” (e.g., when we walk through a doorway; Radvansky and Zacks, 2017). Prior research

suggests that these sharp transitions (termed *event boundaries*) help to discretize our experiences (and their mental representations) into *events* (Radvansky and Zacks, 2017; Brunec et al., 2018; Heusser et al., 2018a; Clewett and Davachi, 2017; Ezzyat and Davachi, 2011; DuBrow and Davachi, 2013). The interplay between the stable (within-event) and transient (across-event) temporal dynamics of an experience also provides a potential framework for transforming experiences into memories that distills those experiences down to their essence. For example, prior work has shown that event boundaries can influence how we learn sequences of items (Heusser et al., 2018a; DuBrow and Davachi, 2013), navigate (Brunec et al., 2018), and remember and understand narratives (Zwaan and Radvansky, 1998; Ezzyat and Davachi, 2011). This work also suggests a means of distinguishing the essence of an experience from its low-level details. The overall structure of events and event transitions reflects how the high-level experience unfolds (i.e., its essence), while subtler event-level properties reflect low-level details. Prior research has also implicated a network of brain regions (including the hippocampus and the medial prefrontal cortex) in playing a critical role in transforming experiences into structured and consolidated memories (Tompry and Davachi, 2017).

Here, we sought to examine how the temporal dynamics of a “naturalistic” experience were later reflected in participants’ memories. We also sought to leverage the above conceptual insights into the distinctions between an experience’s essence and low-level details to build models that explicitly quantified these distinctions. We analyzed an open dataset that comprised behavioral and functional Magnetic Resonance Imaging (fMRI) data collected as participants viewed and then verbally recounted an episode of the BBC television series *Sherlock* (Chen et al., 2017). We developed a computational framework for characterizing the temporal dynamics of the moment-by-moment content of the episode, and of participants’ verbal recalls. Specifically, we use topic modeling (Blei et al., 2003) to characterize the thematic conceptual (semantic) content present in each moment of the episode and recalls, and hidden Markov models (Rabiner, 1989; Baldassano et al., 2017) to discretize this evolving semantic content into events. In this way, we cast both naturalistic experiences and memories of those experiences as geometric *trajectories* that describe how they evolve over time. Under this framework, successful remembering entails verbally “traversing” the content trajectory

99 of the episode, thereby reproducing the shape (essence) of the original experience. Our framework  
100 captures the episode’s essence in the sequence of geometric coordinates for its events, and its  
101 low-level details by examining its within-event geometric properties.

102 Comparing the overall shapes of the topic trajectories for the episode and participants’ recalls  
103 reveals which aspects of the episode’s essence were preserved (or discarded) in the translation into  
104 memory. We also develop two metrics for assessing participants’ memories for low-level details:  
105 (1) the *precision* with which a participant recounts details about each event, and (2) the *distinctiveness*  
106 of each recall event, relative to other recalled events. We examine how these metrics relate to overall  
107 memory performance as judged by third-party human annotators. We also compare and contrast  
108 our general approach to studying memory for naturalistic experiences with standard metrics for  
109 assessing performance on more traditional memory tasks, such as list-learning. Last, we leverage  
110 our framework to identify networks of brain structures whose responses (as participants watched  
111 the episode) reflected the temporal dynamics of either the episode or how participants would later  
112 recount it.

## 113 Results

114 To characterize the dynamic content of the *Sherlock* episode and participants’ subsequent recounts  
115 we used a topic model (Blei et al., 2003) to discover the episode’s latent themes. Topic models  
116 take as inputs a vocabulary of words to consider and a collection of text documents, and return  
117 two output matrices. The first of these is a *topics matrix* whose rows are *topics* (or latent themes)  
118 and whose columns correspond to words in the vocabulary. The entries in the topics matrix  
119 reflect how each word in the vocabulary is weighted by each discovered topic. For example, a  
120 detective-themed topic might weight heavily on words like “crime,” and “search.” The second  
121 output is a *topic proportions matrix*, with one row per document and one column per topic. The  
122 topic proportions matrix describes the mixture of discovered topics reflected in each document.

123 Chen et al. (2017) collected hand-annotated information about each of 1,000 (manually iden-  
124 tified) scenes spanning the roughly 50 minute video used in their experiment. This information

125 included: a brief narrative description of what was happening, the location where the scene took  
126 place, the names of any characters on the screen, and other similar details (for a full list of annotated  
127 features, see *Methods*). We took from these annotations the union of all unique words (excluding  
128 stop words, such as “and,” “or,” “but,” etc.) across all features and scenes as the “vocabulary” for  
129 the topic model. We then concatenated the sets of words across all features contained in overlap-  
130 ping sliding windows of (up to) 50 scenes, and treated each window as a single “document” for  
131 the purpose of fitting the topic model. Next, we fit a topic model with (up to)  $K = 100$  topics to this  
132 collection of documents. We found that 32 unique topics (with non-zero weights) were sufficient to  
133 describe the time-varying content of the episode (see *Methods*; Figs. 1, S2). Note that our approach  
134 is similar in some respects to Dynamic Topic Models (Blei and Lafferty, 2006), in that we sought  
135 to characterize how the thematic content of the episode evolved over time. However, whereas  
136 Dynamic Topic Models are designed to characterize how the properties of *collections* of documents  
137 change over time, our sliding window approach allows us to examine the topic dynamics within  
138 a single document (or video). Specifically, our approach yielded (via the topic proportions matrix)  
139 a single *topic vector* for each sliding window of annotations transformed by the topic model. We  
140 then stretched (interpolated) the resulting windows-by-topics matrix to match the time series of  
141 the 1,976 fMRI volumes collected as participants viewed the episode.

142 The 32 topics we found were heavily character-focused (i.e., the top-weighted word in each topic  
143 was nearly always a character) and could be roughly divided into themes centered around Sherlock  
144 Holmes (the titular character), John Watson (Sherlock’s close confidant and assistant), supporting  
145 characters (e.g., Inspector Lestrade, Sergeant Donovan, or Sherlock’s brother Mycroft), or the  
146 interactions between various groupings of these characters (see Fig. S2). Several of the identified  
147 topics were highly similar, which we hypothesized might allow us to distinguish between subtle  
148 narrative differences if the distinctions between those overlapping topics were meaningful. The  
149 topic vectors for each timepoint were also *sparse*, in that only a small number (typically one or  
150 two) of topics tended to be “active” in any given timepoint (see Fig. 2A). Further, the dynamics  
151 of the topic activations appeared to exhibit *persistence* (i.e., given that a topic was active in one  
152 timepoint, it was likely to be active in the following timepoint) along with *occasional rapid changes*

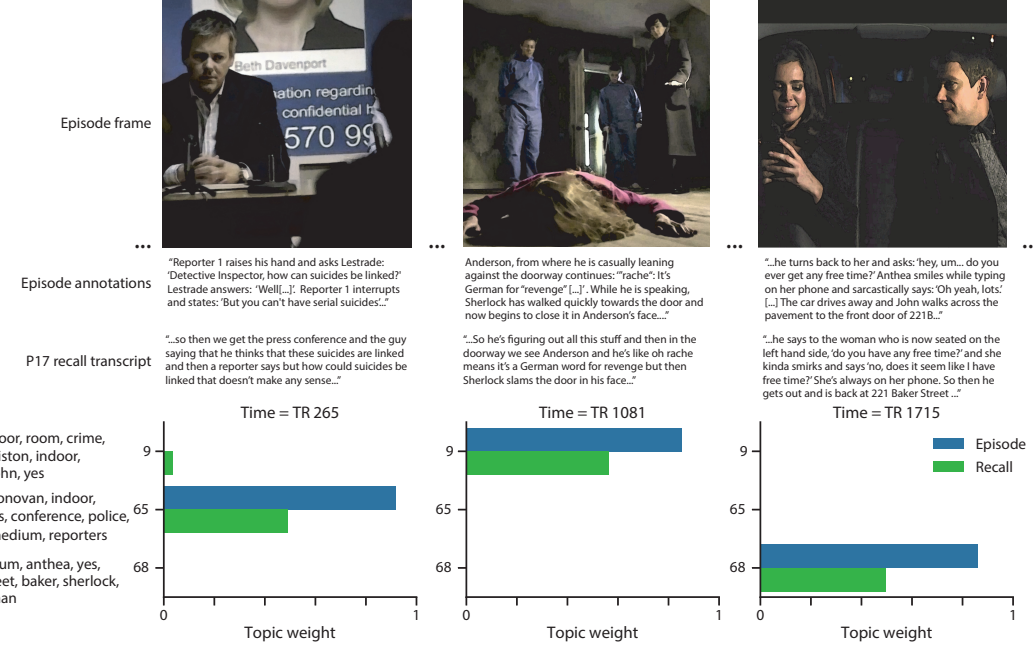


**Figure 1: Topic weights in episode and recall content.** We used hand-annotated descriptions of each manually identified scene from the episode to fit a topic model. Three example episode frames (first row) and their associated descriptions (second row) are displayed. The third row shows an example participant's later recalls of the same three scenes. We used the topic model (fit to the episode annotations) to estimate topic vectors for each moment of the episode and each sentence of participants' recalls. Example topic vectors are displayed in the bottom row (blue: episode annotations; green: example participant's recalls). Three topic dimensions are shown (the highest-weighted topics for each of the three example scenes, respectively), along with the 10 highest-weighted words for each topic. Figure S2 provides a full list of the top 10 words from each of the discovered topics.

153 (i.e., occasionally topics would appear to spring into or out of existence). These two properties  
154 of the topic dynamics may be seen in the block diagonal structure of the timepoint-by-timepoint  
155 correlation matrix (Fig. 2B) and reflect the gradual drift and sudden shifts fundamental to the  
156 temporal dynamics of real-world experiences. Given this observation, we adapted an approach  
157 devised by Baldassano et al. (2017), and used a hidden Markov model (HMM) to identify the *event*  
158 *boundaries* where the topic activations changed rapidly (i.e., the boundaries of the blocks in the  
159 temporal correlation matrix; event boundaries identified by the HMM are outlined in yellow in  
160 Fig. 2B). Part of our model fitting procedure required selecting an appropriate number of “events”  
161 into which the topic trajectory should be segmented. To accomplish this, we used an optimization  
162 procedure that maximized the difference between the topic weights for timepoints within an event  
163 versus timepoints across multiple events (see *Methods* for additional details). We then created a  
164 stable “summary” of the content within each episode event by averaging the topic vectors across  
165 the timepoints spanned by each event (Fig. 2C).

166 Given that the time-varying content of the episode could be segmented cleanly into discrete  
167 events, we wondered whether participants’ recalls of the episode also displayed a similar structure.  
168 We applied the same topic model (already trained on the episode annotations) to each participant’s  
169 recalls. Analogously to how we parsed the time-varying content of the episode, to obtain similar  
170 estimates for each participant’s recall, we treated each overlapping window of (up to 10) sentences  
171 from their transcript as a “document,” and computed the most probable mix of topics reflected in  
172 each timepoint’s sentences. This yielded, for each participant, a number-of-windows by number-of-  
173 topics topic proportions matrix that characterized how the topics identified in the original episode  
174 were reflected in the participant’s recalls. Note that an important feature of our approach is that  
175 it allows us to compare participants’ recalls to events from the original episode, despite different  
176 participants using widely varying language to describe the events, and that those descriptions  
177 often diverged in content and quality from the episode annotations. This is a substantial benefit  
178 of projecting the episode and recalls into a shared “topic” space. An example topic proportions  
179 matrix from one participant’s recalls is shown in Figure 2D.

180 Although the example participant’s recall topic proportions matrix has some visual similarity



**Figure 2: Modeling naturalistic stimuli and recalls.** All panels: darker colors indicate greater values; range: [0, 1]. **A.** Topic vectors ( $K = 100$ ) for each of the 1976 episode timepoints. **B.** Timepoint-by-timepoint correlation matrix of the topic vectors displayed in Panel A. Event boundaries discovered by the HMM are denoted in yellow (30 events detected). **C.** Average topic vectors for each of the 30 episode events. **D.** Topic vectors for each of 265 sliding windows of sentences spoken by an example participant while recalling the episode. **E.** Timepoint-by-timepoint correlation matrix of the topic vectors displayed in Panel D. Event boundaries detected by the HMM are denoted in yellow (22 events detected). For similar plots for all participants, see Figure S4. **F.** Average topic vectors for each of the 22 recall events from the example participant. **G.** Correlations between the topic vectors for every pair of episode events (Panel C) and recall events (from the example participant; Panel F). For similar plots for all participants, see Figure S5. **H.** Average correlations between each pair of episode events and recall events (across all 17 participants). To create the figure, each recalled event was assigned to the episode event with the most correlated topic vector (yellow boxes in panels G and H).

181 to the episode topic proportions matrix, the time-varying topic proportions for the example par-  
182 ticipant's recalls are not as sparse as those for the episode (compare Figs. 2A and D). Similarly,  
183 although there do appear to be periods of stability in the recall topic dynamics (i.e., most topics are  
184 active or inactive over contiguous blocks of time), the changes in topic activations that define event  
185 boundaries appear less clearly delineated in participants' recalls than in the episode's annotations.  
186 To examine these patterns in detail, we computed the timepoint-by-timepoint correlation matrix for  
187 the example participant's recall trajectory (Fig. 2E). As in the episode correlation matrix (Fig. 2B),  
188 the example participant's recall correlation matrix has a strong block diagonal structure, indicating  
189 that their recalls are discretized into separated events. As for the episode correlation matrix, we  
190 leveraged an HMM-based optimization procedure (see *Methods*) to determine how many events  
191 are reflected in the participant's recalls and where specifically the event boundaries fall (outlined  
192 in yellow). We carried out a similar analysis on all 17 participants' recall topic proportions matrices  
193 (Fig. S4).

194 Two clear patterns emerged from this set of analyses. First, although every individual partic-  
195 ipant's recalls could be segmented into discrete events (i.e., every individual participant's recall  
196 correlation matrix exhibited clear block diagonal structure; Fig. S4), each participant appeared to  
197 have a unique *recall resolution*, reflected in the sizes of those blocks. While some participants' recall  
198 topic proportions segmented into just a few events (e.g., Participants P4, P5, and P7), others' seg-  
199 mented into many shorter duration events (e.g., Participants P12, P13, and P17). This suggests that  
200 different participants may be recalling the episode with different levels of detail—i.e., some might  
201 touch on just the major plot points, whereas others might attempt to recall every minor scene or  
202 action. The second clear pattern present in every individual participant's recall correlation matrix  
203 was that, unlike in the episode correlation matrix, there were substantial off-diagonal correlations.  
204 Whereas each event in the original episode was (largely) separable from the others (Fig. 2B), in  
205 transforming those separable events into memory, participants appeared to be integrating across  
206 multiple events, blending elements of previously recalled and not-yet-recalled content into each  
207 newly recalled event (Figs. 2E, S4; also see Manning et al., 2011; Howard et al., 2012; Manning,  
208 2019).

209 The above results indicate that both the structure of the original episode and participants' recalls  
210 of the episode exhibit event boundaries that can be identified automatically by characterizing the  
211 dynamic content using a shared topic model and segmenting the content into events via HMMs.  
212 Next, we asked whether some correspondence might be made between the specific content of the  
213 events the participants experienced in the episode, and the events they later recalled. One approach  
214 to linking the experienced (episode) and recalled events is to label each recalled event as matching  
215 the episode event with the most similar (i.e., most highly correlated) topic vector (Figs. 2G, S5). This  
216 yields a sequence of "presented" events from the original episode, and a (potentially differently  
217 ordered) sequence of "recalled" events for each participant. Analogous to classic list-learning  
218 studies, we can then examine participants' recall sequences by asking which events they tended  
219 to recall first (probability of first recall; Fig. 3A; Atkinson and Shiffrin, 1968; Postman and Phillips,  
220 1965; Welch and Burnett, 1924); how participants most often transition between recalls of the  
221 events as a function of the temporal distance between them (lag-conditional response probability;  
222 Fig. 3B; Kahana, 1996); and which events they were likely to remember overall (serial position  
223 recall analyses; Fig. 3C; Murdock, 1962). Interestingly, for two of these analyses (probability of  
224 first recall and lag-conditional response probability curves) we observed patterns comparable to  
225 classic effects from list-learning literature: namely, a higher probability of initiating recall with the  
226 first event in the sequence (Fig. 3A) and a higher probability of transitioning to neighboring events  
227 with an asymmetric forward bias (Fig. 3B). In contrast, we did not observe a pattern comparable  
228 to the serial position effect (Fig. 3C), but rather greater memory for specific events distributed  
229 approximately evenly throughout the episode.

230 We can also apply two list-learning-native analyses that describe how participants group items  
231 in their recall sequences: temporal clustering and semantic clustering (Polyn et al., 2009, see  
232 *Methods* for details). Temporal clustering refers to the extent to which participants group their  
233 recall responses according to encoding position. Overall, we found that sequentially viewed  
234 episode events were clustered heavily in participants' recall event sequences (mean clustering  
235 score: 0.767, SEM: 0.029), and that participants with higher temporal clustering scores tended to  
236 perform better according to both Chen et al. (2017)'s hand-annotated memory scores (Pearson's

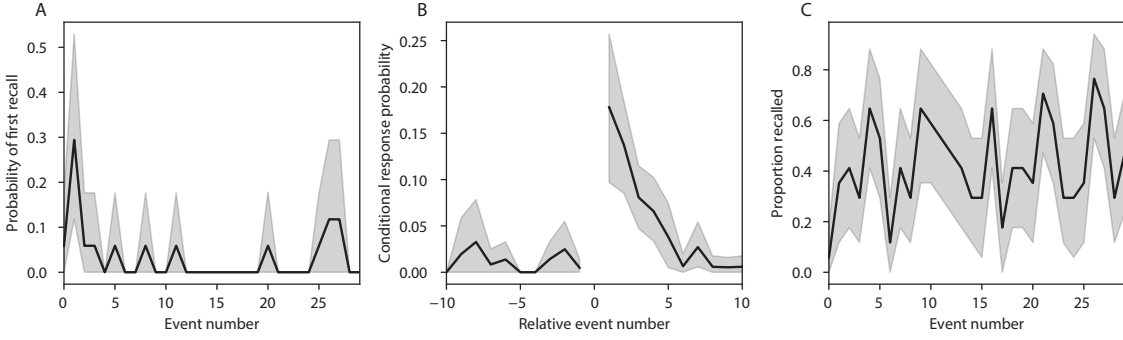


**Figure 3: Naturalistic extensions of classic list-learning memory analyses.** **A.** The probability of first recall as a function of the serial position of the event in the episode. **B.** The probability of recalling each event, conditioned on having most recently recalled the event *lag* events away in the episode. **C.** The proportion of participants who recalled each event, as a function of the serial position of the events in the episode. All panels: error ribbons denote bootstrap-estimated standard error of the mean.

237  $r(15) = 0.62, p = 0.008$ ) and our model's estimate (Pearson's  $r(15) = 0.54, p = 0.024$ ). Semantic  
 238 clustering measures the extent to which participants cluster their recall responses according to  
 239 semantic similarity. We found that participants tended to recall semantically similar episode  
 240 events together (mean clustering score: 0.787, SEM: 0.018), and that semantic clustering score  
 241 was also related to both hand-annotated (Pearson's  $r(15) = 0.65, p = 0.004$ ) and model-derived  
 242 (Pearson's  $r(15) = 0.63, p = 0.007$ ) memory performance.

243 Statistical models of memory studies often treat recall success as binary (in other words, an  
 244 item either was or was not recalled), or occasionally categorical (e.g., to distinguish familiarity  
 245 from recollection; Yonelinas et al., 2002). Such approaches are tenable in classical list-learning or  
 246 recognition memory paradigms, as the presented stimuli tend to be very simple (e.g., a sequence of  
 247 individual words or items). However, memory for naturalistic experiences is much more nuanced.  
 248 For example, certain aspects of an experience might be correctly remembered at varying levels of  
 249 detail, or distorted, or forgotten entirely. Further, each remembering is itself a richly structured  
 250 phenomenon. Our framework produces a content-based model of individual episode and recall  
 251 events by projecting the dynamic content of the episode and participants' recalls into a shared  
 252 topic space. This allows for direct, quantitative comparisons between all stimulus and recall  
 253 events, as well as between the recall events themselves. Leveraging these content-based models of

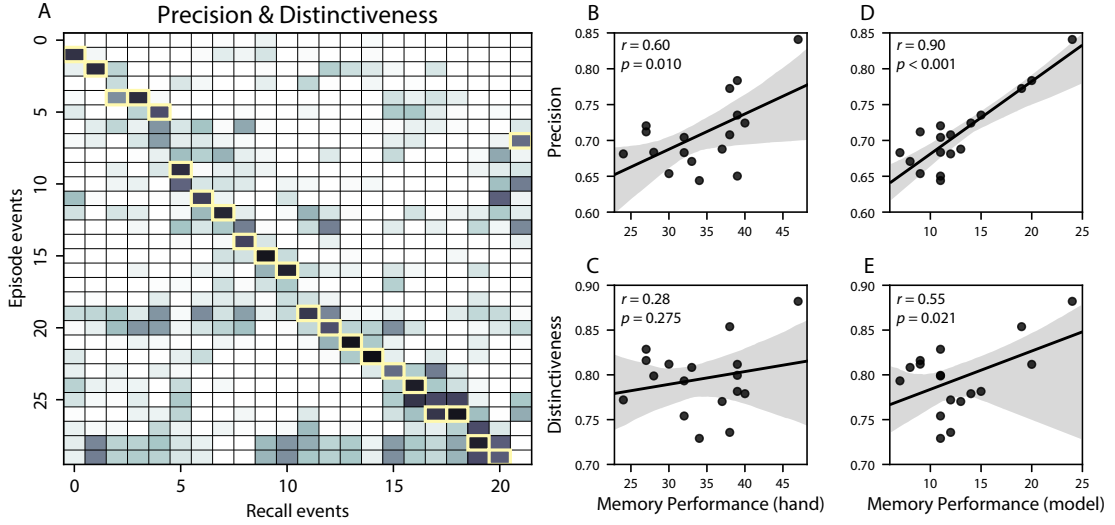


**Figure 4: Novel content-based metrics of naturalistic memory: precision and distinctiveness.** A. The episode-recall correlation matrix for a representative participant (17). The yellow boxes highlight the maximum correlation in each column. The example participant's overall precision score was computed as the average across correlation values in the yellow boxes. Their distinctiveness score was computed as the average (over recall events) of 1 minus the average correlation between each recall event and all other recall events that do not display a box in the same row. B. The (Pearson's) correlation between precision and hand-annotated memory performance. C. The correlation between distinctiveness and hand-annotated memory performance. D. The correlation between precision and the number of episode events successfully recalled, as determined by our model. E. The correlation between distinctiveness and the number of episode events successfully recalled, as determined by our model.

the stimulus/recall events, we developed two novel, *continuous* metrics for analyzing naturalistic memory: *precision* and *distinctiveness*. Precision is intended to capture the “completeness” of recall, or how fully the presented content was recapitulated in memory. We define a recall event’s precision as the maximum correlation between the topic proportions of that recall event and any episode event (Fig. 4). A second novel metric we introduce here is *distinctiveness*, which is intended to capture the “specificity” of recall. In other words, distinctiveness quantifies the extent to which a given recalled event reflects the most similar presented event more so than it does other presented events. To compute a recall event’s distinctiveness, we first identify the episode event to which its topic vector is most strongly correlated. We then define distinctiveness as one minus the average correlation between the given recall event and all *other* episode events.

264 In addition to individual events, one may also use these metrics to describe each participant's  
265 overall performance by averaging across a participant's event-wise precision or distinctiveness  
266 scores. Participants whose recall events are more veridical descriptions of what happened in the  
267 episode event will presumably have higher precision scores. We find that, across participants,  
268 higher precision scores are positively correlated with both hand-annotated memory performance  
269 (as collected by Chen et al., 2017; Pearson's  $r(15) = 0.60, p = 0.010$ ) and the number of episode  
270 events successfully remembered, as determined by our model (Pearson's  $r(15) = 0.90, p < 0.001$ ).  
271 We also hypothesized that participants who recounted events in a more distinctive way would  
272 display better overall memory. We find that participants' distinctiveness scores were positively  
273 correlated with our model's estimated number of recall events (Pearson's  $r(15) = 0.55, p = 0.021$ ).  
274 However, we found no evidence that distinctiveness scores were correlated with hand-annotated  
275 memory performance (Pearson's  $r(15) = 0.28, p = 0.275$ ). We elaborate on this potential discrepancy  
276 in the *Discussion* section.

277 Further intuition for the behaviors captured by these two metrics may be gained by directly  
278 examining the content of the episode and recalls our framework models. In Figure 5, we contrast  
279 recalls for the same episode event (event 22) from two participants: one with a high precision  
280 score (P17), the other with a low precision score (P6). From the HMM-identified event boundaries,  
281 we recovered the set of annotations describing the content of an example episode event (Fig. 5B),  
282 and divided them into different color-coded sections for each action or feature described. We  
283 then similarly recovered the set of sentences comprising the corresponding recall event for each  
284 of the two example participants. Because the recall sliding windows overlap heavily, and each  
285 recall event spans multiple recall timepoints (i.e., windows), we have stripped any sentences from  
286 the beginning and end that describe earlier or later episode events for the sake of readability. In  
287 other words, Fig. 5C shows a subset of the full recall event text, comprising sentences between the  
288 first and last descriptions of content from the example episode event. We then colored all words  
289 describing actions and features coded in panel B by their corresponding color. Visual comparison  
290 of these example transcripts reveals that the more precise recall captures more of the episode  
291 event's content, and with more detail.

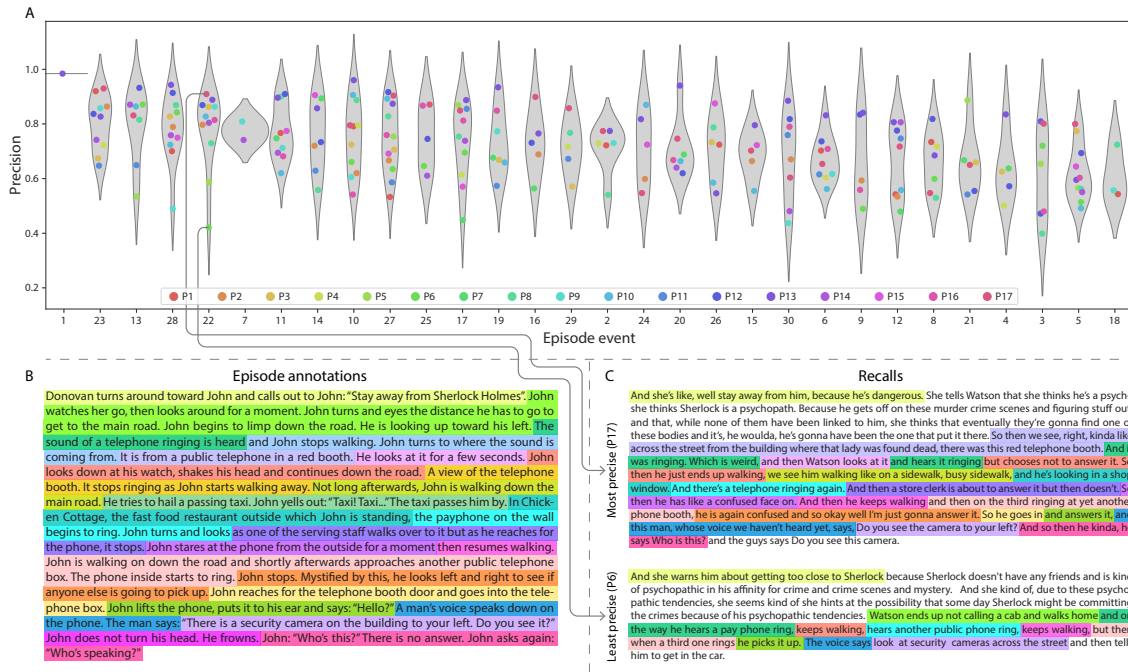


**Figure 5: Precision metric reflects completeness of recall.** **A.** Recall precision by episode event. Grey violin plots display kernel density estimates for the distribution of recall precision scores for a single episode event. Colored dots within each violin plot represent individual participants' recall precision for the given event. Episode events are ordered along the x-axis by the average precision with which they were remembered. **B.** The set of "Narrative Details" episode annotations (generated by Chen et al., 2017) for scenes comprising an example episode event (22) identified by the HMM. Each action or feature is highlighted in a different color. **C.** A subset of the sentences comprising the most precise (P17) and least precise (P6) participants' recalls of episode event 22. Descriptions of specific actions or features reflecting those highlighted in panel B are highlighted in the corresponding color.

292     Figure 6 similarly contrasts two example participants' recalls for a common episode event (event  
 293     19) to illustrate the tangible differences between high and low distinctiveness scores. Here, we  
 294     have extracted the full set of sentences comprising the most distinctive recall event (P13) and least  
 295     distinctive recall event (P11) matched to the example episode event (Fig. 6C). We also extracted  
 296     the annotations for the example episode event, as well as those from each other episode event  
 297     whose content the example participants' single recall events described (Fig. 6B). We then shaded  
 298     the annotation text for each episode event with a different color, and shaded each word of the  
 299     example participants' recall text by the color of the episode event it describes. The majority of  
 300     the most distinctive recall event text describes episode event 19's content, with the first five and

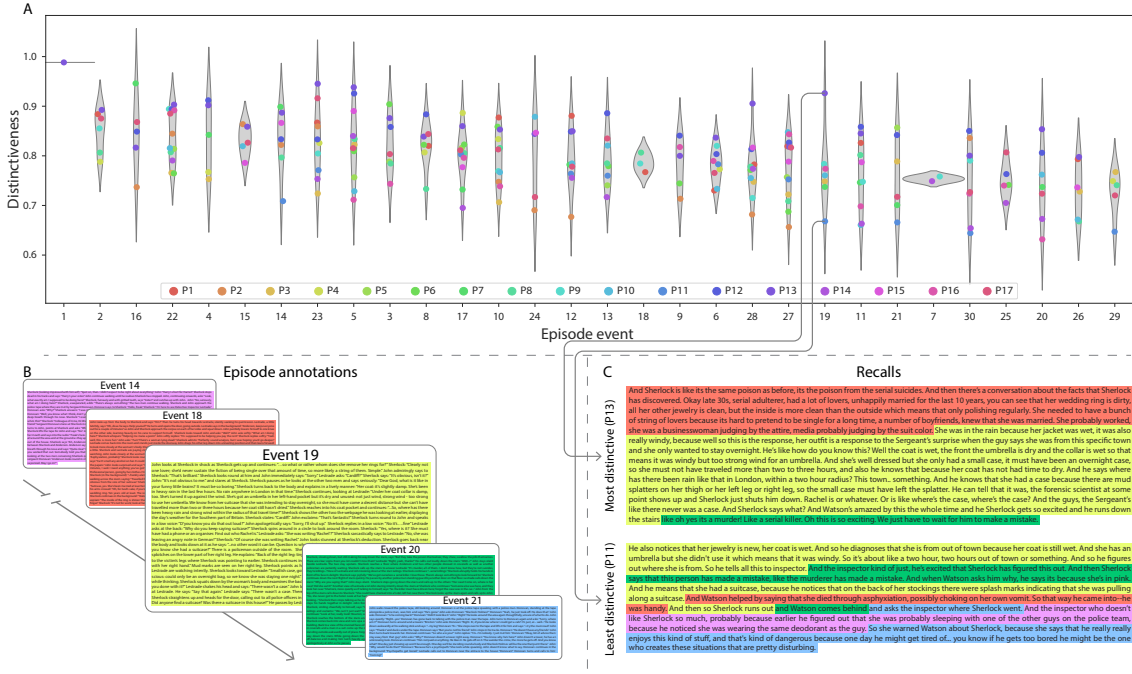


**Figure 6: Distinctiveness metric reflects specificity of recall.** A. Recall distinctiveness by episode event. Kernel density estimates for each episode event’s distribution of recall distinctiveness scores, analogous to Fig. 5A. B. The sets of “Narrative Details” episode annotations (generated by Chen et al., 2017) for scenes comprising episode events described by the example participants in panel C. Each event’s text is highlighted in a different color. C. The sentences comprising the most distinctive (P13) and least distinctive (P11) participants’ recalls of episode event 19. Sections of recall describing each episode event in panel B are highlighted with the corresponding color.

301 last one sentence describing the episode events immediately preceding and succeeding the current  
302 one, respectively. In contrast, the least distinctive recall of episode event 19 blends the content  
303 from five separate episode events, does not transition between them in order, and often combines  
304 descriptions of two episode events' content in the same sentence.

The prior analyses leverage the correspondence between the 100-dimensional topic proportion matrices for the episode and participants' recalls to characterize recall. However, it is difficult to gain deep insights into the content of (or relationships between) experiences and memories solely by examining these topic proportions (e.g., Figs. 2A, D) or the corresponding correlation matrices (Figs. 2B, E, S4). And while we can directly examine the original text underlying these topic vectors (e.g., Figs. 5, 6) to show how relationships between them reflect real-world behavior, this

311 comparison becomes prohibitively cumbersome at larger timescales. To visualize the time-varying  
312 high-dimensional content in a more intuitive way (Heusser et al., 2018b), we projected the topic  
313 proportions matrices onto a two-dimensional space using Uniform Manifold Approximation and  
314 Projection (UMAP; McInnes et al., 2018). In this lower-dimensional space, each point represents a  
315 single episode or recall event, and the distances between the points reflect the distances between  
316 the events' associated topic vectors (Fig. 7). In other words, events that are nearer to each other in  
317 this space are more semantically similar, and those that are farther apart are less so.

318 Visual inspection of the episode and recall topic trajectories reveals a striking pattern. First,  
319 the topic trajectory of the episode (which reflects its dynamic content; Fig. 7A) is captured nearly  
320 perfectly by the averaged topic trajectories of participants' recalls (Fig. 7B). To assess the consis-  
321 tency of these recall trajectories across participants, we asked: given that a participant's recall  
322 trajectory had entered a particular location in the reduced topic space, could the position of their  
323 *next* recalled event be predicted reliably? For each location in the the reduced topic space, we  
324 computed the set of line segments connecting successively recalled events (across all participants)  
325 that intersected that location (see *Methods* for additional details). We then computed (for each  
326 location) the distribution of angles formed by the lines defined by those line segments and a fixed  
327 reference line (the *x*-axis). Rayleigh tests revealed the set of locations in topic space at which these  
328 across-participant distributions exhibited reliable peaks (blue arrows in Fig. 7B reflect significant  
329 peaks at  $p < 0.05$ , corrected). We observed that the locations traversed by nearly the entire episode  
330 trajectory exhibited such peaks. In other words, participants exhibited similar trajectories that also  
331 matched the trajectory of the original episode (Fig. 7C). This is especially notable when considering  
332 the fact that the number of events participants recalled (dots in Fig. 7C) varied considerably across  
333 people, and that every participant used different words to describe what they had remembered  
334 happening in the episode. Differences in the numbers of remembered events appear in partici-  
335 pants' trajectories as differences in the sampling resolution along the trajectory. We note that this  
336 framework also provides a means of disentangling classic "proportion recalled" measures (i.e.,  
337 the proportion of episode events described in participants' recalls) from participants' abilities to  
338 recapitulate the overall unfolding of the original episode's content (i.e., the similarity between the

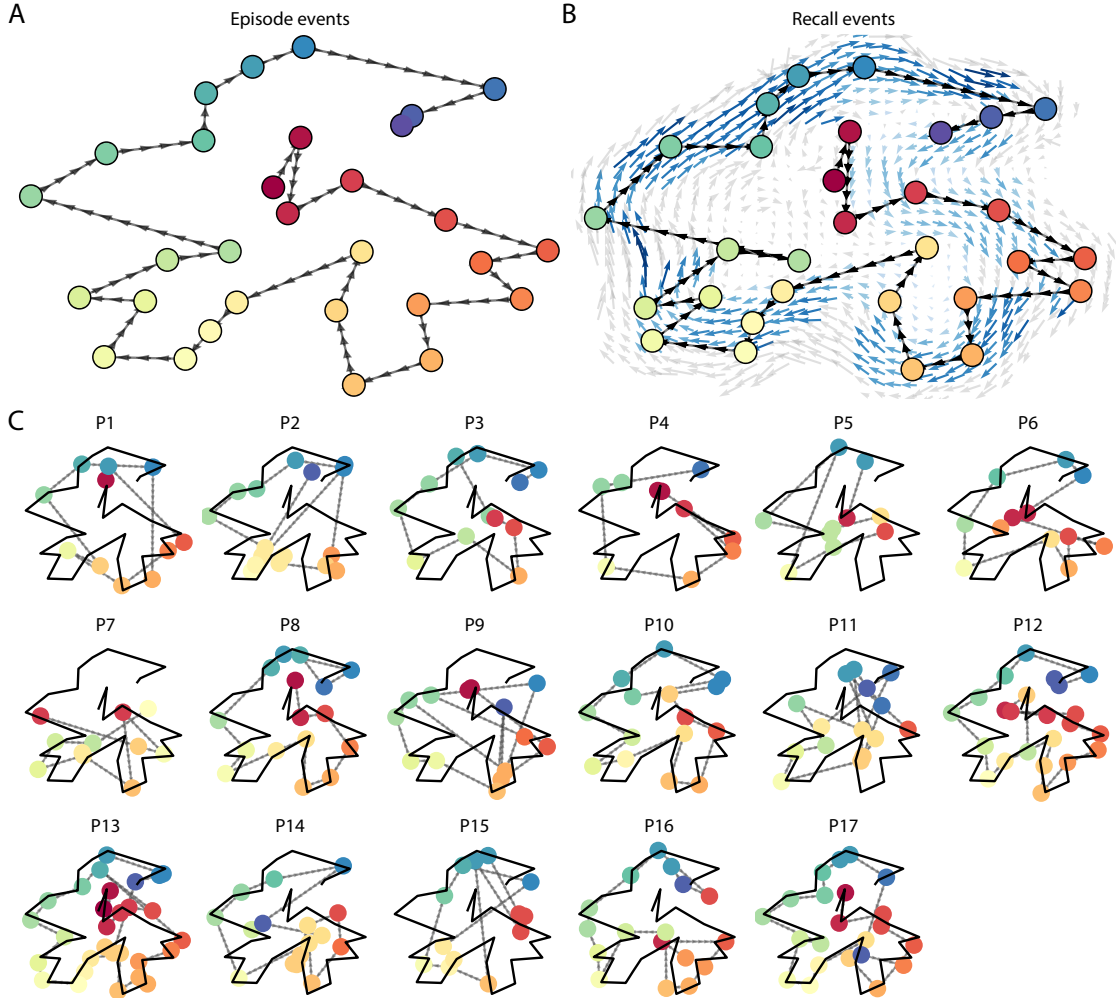


**Figure 7: Trajectories through topic space capture the dynamic content of the episode and recalls.** All panels: the topic proportion matrices have been projected onto a shared two-dimensional space using UMAP. **A.** The two-dimensional topic trajectory taken by the episode of *Sherlock*. Each dot indicates an event identified using the HMM (see *Methods*); the dot colors denote the order of the events (early events are in red; later events are in blue), and the connecting lines indicate the transitions between successive events. **B.** The average two-dimensional trajectory captured by participants' recall sequences, with the same format and coloring as the trajectory in Panel A. To compute the event positions, we matched each recalled event with an event from the original episode (see *Results*), and then we averaged the positions of all events with the same label. The arrows reflect the average transition direction through topic space taken by any participants whose trajectories crossed that part of topic space; blue denotes reliable agreement across participants via a Rayleigh test ( $p < 0.05$ , corrected). **C.** The recall topic trajectories (gray) taken by each individual participant (P1–P17). The episode's trajectory is shown in black for reference. Here, events (dots) are colored by their matched episode event (Panel A).

339 shapes of the original episode trajectory and that defined by each participant's recounting of the  
340 episode).

341 In addition to the more "holistic" measure of memory described in the previous section, our  
342 framework also affords the ability to drill down to individual words and quantify how each word  
343 relates to the memorability of each event. The results displayed in Figures 3C and 5A suggest that  
344 certain events were remembered better than others. Given this, we next asked whether the  
345 events were generally remembered well or poorly tended to reflect particular content. Because our  
346 analysis framework projects the dynamic episode content and participants' recalls into a shared  
347 space, and because the dimensions of that space represent topics (which are, in turn, sets of weights  
348 over known words in the vocabulary), we are able to recover the weighted combination of words  
349 that make up any point (i.e., topic vector) in this space. We first computed the average precision  
350 with which participants recalled each of the 30 episode events (Fig. 8A; note that this result is  
351 analogous to a serial position curve created from our continuous recall quality metric). We then  
352 computed a weighted average of the topic vectors for each episode event, where the weights  
353 reflected how reliably each event was recalled. To visualize the result, we created a "wordle"  
354 image (Mueller et al., 2018) where words weighted more heavily by better-remembered topics  
355 appear in a larger font (Fig. 8B, green box). Across the full episode, content that reflected topics  
356 necessary to convey the central focus of the episode (e.g., the names of the two main characters,  
357 "Sherlock" and "John," and the address of a major recurring location, "221B Baker Street") were  
358 best remembered. An analogous analysis revealed which themes were poorly remembered. Here  
359 in computing the weighted average over events' topic vectors, we weighted each event in *inverse*  
360 proportion to how well it was remembered (Fig. 8B, red box). The least well-remembered episode  
361 content reflected information not necessary to later convey a general summary of the episode, such  
362 as the proper names of relatively minor characters (e.g., "Mike," "Molly," and "Lestrade") and  
363 locations (e.g., "St. Bartholomew's Hospital").

364 A similar result emerged from assessing the topic vectors for individual episode and recall  
365 events (Fig. 8C). Here, for each of the three best- and worst-remembered episode events, we have  
366 constructed two wordles: one from the original episode event's topic vector (left) and a second

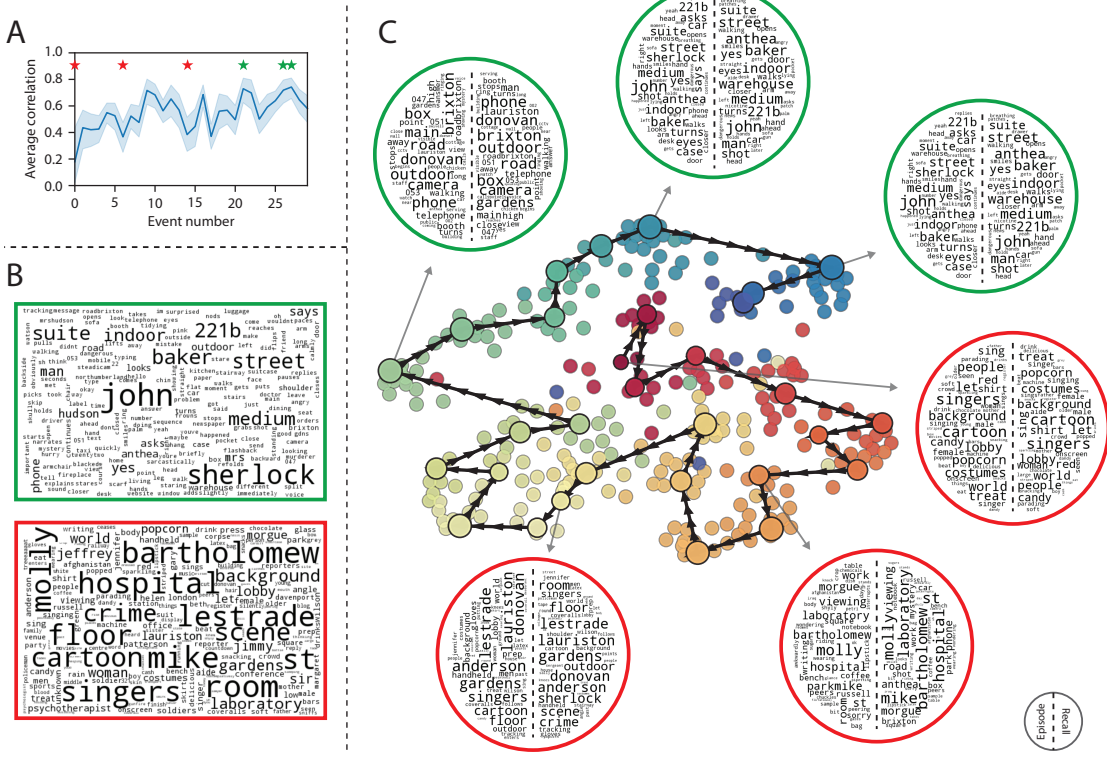


**Figure 8: Language used in the most and least memorable events.** **A.** Average precision (episode event-recall event topic vector correlation) across participants for each episode event. Error bars denote bootstrap-derived across-participant 95% confidence intervals. The stars denote the three best-remembered events (green) and worst-remembered events (red). **B.** Wordles comprising the top 200 highest-weighted words reflected in the weighted-average topic vector across episode events. Green: episode events were weighted by how well the topic vectors derived from recalls of those events matched the episode events' topic vectors (Panel A). Red: episode events were weighted by the inverse of how well their topic vectors matched the recalled topic vectors. **C.** The set of all episode and recall events is projected onto the two-dimensional space derived in Figure 7. The dots outlined in black denote episode events (dot size reflects the average correlation between the episode event's topic vector and the topic vectors from the closest matching recalled events from each participant; bigger dots denote stronger correlations). The dots without black outlines denote recalled events. All dots are colored using the same scheme as Figure 7A. Wordles for several example events are displayed (green: three best-remembered events; red: three worst-remembered events). Within each circular wordle, the left side displays words associated with the topic vector for the episode event, and the right side displays words associated with the (average) recall event topic vector, across all recall events matched to the given episode event.

367 from the average recall topic vector for that event (right). The three best-remembered events  
368 (circled in green) correspond to scenes integral to the central plot-line: a mysterious figure spying  
369 on John in a phone booth; John meeting Sherlock at Baker St. to discuss the murders; and Sherlock  
370 laying a trap to catch the killer. Meanwhile, the three worst-remembered events (circled in red)  
371 reflect scenes that are non-essential to summarizing the narrative's structure: the video of singing  
372 cartoon characters participants viewed in an introductory clip prior to the main episode; John  
373 asking Molly about Sherlock's habit of over-analyzing people; and Sherlock noticing evidence of  
374 Anderson's and Donovan's affair.

375 The results thus far inform us about which aspects of the dynamic content in the episode partic-  
376 ipants watched were preserved or altered in participants' memories. We next carried out a series  
377 of analyses aimed at understanding which brain structures might facilitate these preservations  
378 and transformations between the external world and memory. In the first analysis, we sought to  
379 identify brain structures that were sensitive to the dynamic unfolding of the episode's content,  
380 as characterized by its topic trajectory. We used a searchlight procedure to identify clusters of  
381 voxels whose activity patterns displayed a proximal temporal correlation structure (as participants  
382 watched the episode) matching that of the original episode's topic proportions (Fig. 9A; see *Methods*  
383 for additional details). In a second analysis, we sought to identify brain structures whose responses  
384 (during episode viewing) reflected how each participant would later structure their recounting of  
385 the episode. We used an analogous searchlight procedure to identify clusters of voxels whose  
386 proximal temporal correlation matrices matched that of the topic proportions for each individual's  
387 recall (Figs. 9B; see *Methods* for additional details). To ensure our searchlight procedure identified  
388 regions *specifically* sensitive to the temporal structure of the episode or recalls (i.e., rather than those  
389 with a temporal autocorrelation length similar to that of the episode/recalls), we performed a phase  
390 shift-based permutation correction (see *Methods* for additional details). As shown in Figure 9C,  
391 the episode-driven searchlight analysis revealed a distributed network of regions that may play  
392 a role in processing information relevant to the narrative structure of the episode. Similarly, the  
393 recall-driven searchlight analysis revealed a second network of regions (Fig. 9D) that may facilitate  
394 a person-specific transformation of one's experience into memory. In identifying regions whose

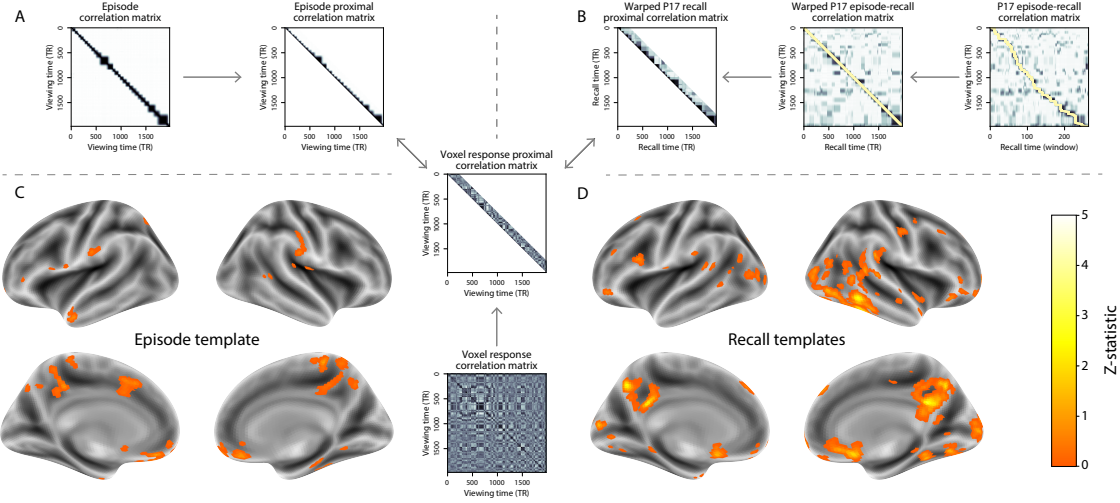


**Figure 9: Brain structures that underlie the transformation of experience into memory.** **A.** We isolated the proximal diagonals from the upper triangle of the episode correlation matrix, and applied this same diagonal mask to the voxel response correlation matrix for each cube of voxels in the brain. We then searched for brain regions whose activation timeseries consistently exhibited a similar proximal correlational structure to the episode model, across participants. **B.** We used dynamic time warping (Berndt and Clifford, 1994) to align each participant’s recall timeseries to the TR timeseries of the episode. We then applied the same diagonal mask used in Panel A to isolate the proximal temporal correlations and searched for brain regions whose activation timeseries for an individual consistently exhibited a similar proximal correlational structure to each individual’s recall. **C.** We identified a network of regions sensitive to the narrative structure of participants’ ongoing experience. The map shown is thresholded at  $p < 0.05$ , corrected. **D.** We also identified a network or regions sensitive to how individuals would later structure the episode’s content in their recalls. The map shown is thresholded at  $p < 0.05$ , corrected.

395 responses to ongoing experiences reflect how those experiences will be remembered later, this  
 396 latter analysis extends classic *subsequent memory analyses* (e.g., Paller and Wagner, 2002) to domain  
 397 of naturalistic stimuli.

398 The searchlight analyses described above yielded two distributed networks of brain regions,  
 399 whose activity timecourses mirrored to the temporal structure of the episode (Fig. 9C) or partic-  
 400 ipants’ eventual recalls (Fig. 9D). We next sought to gain greater insight into the structures and  
 401 functional networks our results reflected. To accomplish this, we performed an additional, ex-  
 402 ploratory analysis using Neurosynth (Yarkoni et al., 2011). Given an arbitrary statistical map as  
 403 input, Neurosynth performs a massive automated meta-analysis, returning a ranked list of terms  
 404 reported in papers with similar significance maps. We ran Neurosynth on the significance maps

<sup>405</sup> for the episode- and recall-driven searchlight analyses. These maps, along with the 10 terms with  
<sup>406</sup> maximally similar meta-analysis images identified by Neurosynth are shown in Figure 10.

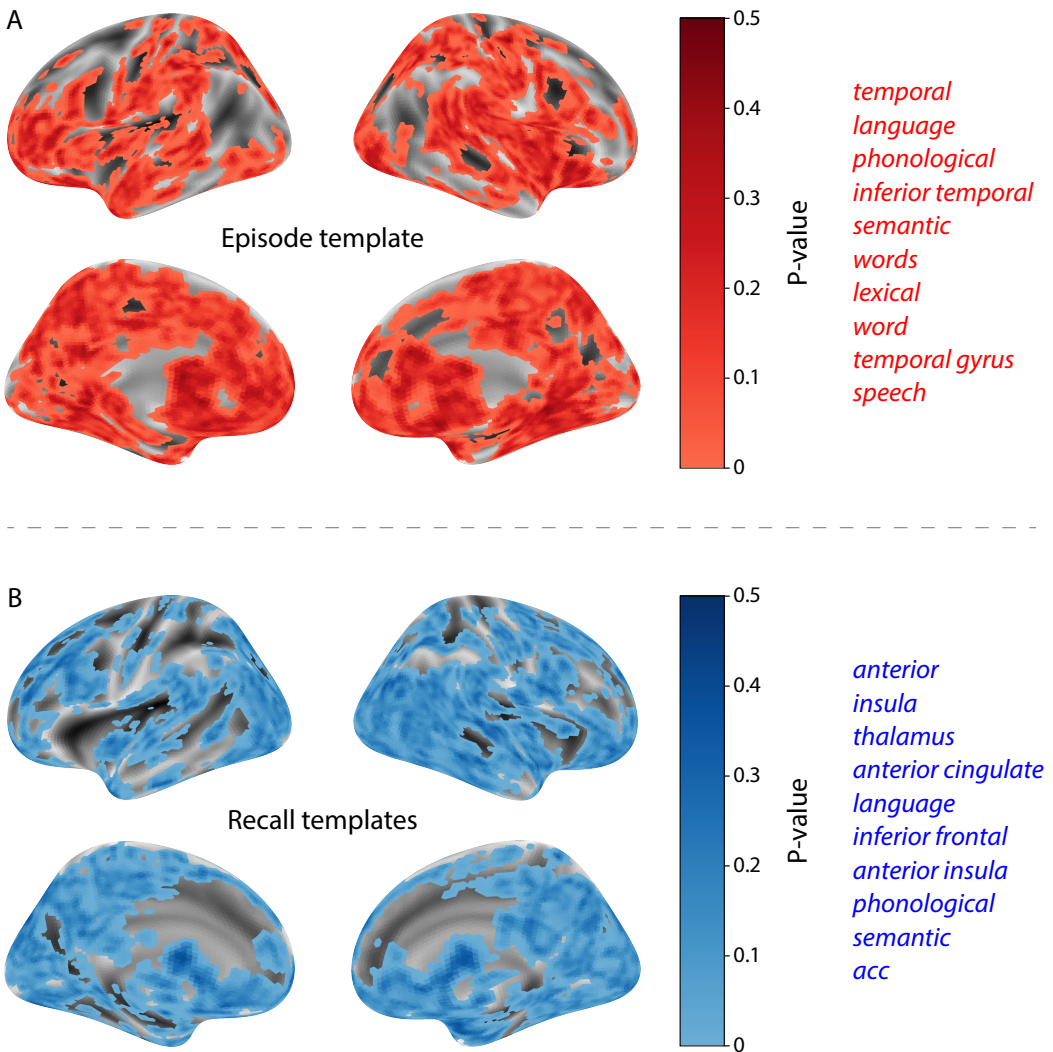


**Figure 10: Decoding distributed statistical maps via Neurosynth meta-analyses.** A. episode-searchlight significance and top 10 decoded terms. We constructed a map of the permutation-derived  $p$ -values for the episode-driven searchlight analysis (Fig. 9A, C) at each voxel with a positive permutation-derived  $z$ -score. The top 10 terms decoded from this significance map are shown in red. B. Recall-searchlight significance and top 10 decoded terms. We constructed a map of the permutation-derived  $p$ -values for the recall-driven searchlight analysis (Fig. 9A, C) at each voxel with a positive permutation-derived  $z$ -score. The top 10 terms decoded from this significance map are shown in blue.

407 **Discussion**

408 Our work casts remembering as reproducing (behaviorally and neurally) the topic trajectory, or  
409 shape, of an experience. This view draws inspiration from prior work aimed at elucidating  
410 the neural and behavioral underpinnings of how we process dynamic naturalistic experiences  
411 and remember them later. One approach to identifying neural responses to naturalistic stimuli  
412 (including experiences) entails building a model of the stimulus and searching for brain regions  
413 whose responses are consistent with the model. In prior work, a series of studies from Uri Hasson's  
414 group (Lerner et al., 2011; Simony et al., 2016; Chen et al., 2017; Baldassano et al., 2017; Zadbood  
415 et al., 2017) have extended this approach with a clever twist: rather than building an explicit  
416 stimulus model, these studies instead search for brain responses (while experiencing the stimulus)  
417 that are reliably similar across individuals. So called *inter-subject correlation* (ISC) and *inter-subject*  
418 *functional connectivity* (ISFC) analyses effectively treat other people's brain responses to the stimulus  
419 as a "model" of how its features change over time. By contrast, in our present work, we use topic  
420 models to construct an explicit content model directly from the stimulus (i.e., the topic trajectory  
421 of the episode). Projecting each participant's recall into a space shared by both the stimulus and  
422 other participants then allows us to compare recalls both directly to the stimulus and to each other.  
423 Similarly, prior work introducing the use of HMMs to discover latent event structure in naturalistic  
424 stimuli and recall (Baldassano et al., 2017) used between-subjects cross-validation to identify event  
425 boundaries shared across participants, and between stimulus and recall. Our framework allows  
426 us to break from the restriction of a common, shared event-timeseries and identify the unique  
427 *resolution* of each participant's recall event structure, and how that may differ from the episode and  
428 that of other participants.

429 Word embedding models are a rapidly growing area of machine learning research. Early ap-  
430 proaches including latent semantic analysis (Landauer and Dumais, 1997) use word co-occurrence  
431 statistics (i.e., how often pairs of words occur in the same documents contained in the corpus) to  
432 derive a unique feature vector for each word. The feature vectors are constructed so that words  
433 that co-occur more frequently have feature vectors that are closer (in Euclidean distance). Related

434 approaches, such as latent dirichlet allocation (Blei et al., 2003) attempt to explicitly model the  
435 underlying causes of word co-occurrences by automatically identifying the set of themes or topics  
436 reflected across the documents in the corpus. More recent work on these types of semantic mod-  
437 els, including word2vec (Mikolov et al., 2013), the Universal Sentence Encoder (Cer et al., 2018),  
438 GPT-2 (Radford et al., 2019), and GTP-3 (Brown et al., 2020) use deep neural networks to attempt  
439 to identify the deeper conceptual representations underlying each word. Despite the growing  
440 popularity of more sophisticated deep learning-based embedding models, here we leverage latent  
441 dirichlet allocation (i.e., topic modeling) to embed episode and recall text. This decision was mo-  
442 tivated by several factors. First, topic models capture the *essence* of a text passage devoid of the  
443 specific set and order of words used. This was an important feature of our model since different  
444 people may accurately recall a scene using very different language. Second, words can mean  
445 different things in different contexts (e.g. “bat” may be the act of hitting a baseball, the object used  
446 for that action, or as a flying mammal). Topic models are robust to this, allowing words to exist  
447 as part of multiple topics. Last, topic models provide a straightforward means of recovering the  
448 weights for the particular words comprising a topic, enabling straightforward interpretation of an  
449 event’s contents (e.g. Fig. 8). Other models such as the Universal Sentence Encoder, GPT-2, and  
450 GPT-3 offer context-sensitive encoding of text passages, but the encoding space is complex and  
451 non-linear, and thus recovering the original words used to fit the model is not straightforward.  
452 However, it is worth pointing out that our general framework is divorced from the particular  
453 choice of language model. Moreover, many of the aspects of our framework could be swapped  
454 out for other choices. For example, the language model, the timeseries segmentation model and  
455 the episode-recall matching function could all be customized to suit a particular question space  
456 or application. Indeed for some questions, recovery of the particular words used to describe  
457 a memory may not be necessary, and thus other text-modeling approaches (including the deep  
458 learning-based embedding models described above) may be preferable. Future work will explore  
459 the influence of particular model choices on the framework’s efficacy.

460 In extending classical free recall analyses to our naturalistic memory framework, we recovered  
461 two patterns of recall dynamics central to list-learning studies: a heightened probability of initiating

recall with the first presented “item” (in our case, episode events; Fig. 3A) and a strong bias toward transitioning from recalling a given event to recalling the one immediately following it (Fig. 3B). However, equally noteworthy are the typical free recall results *not* recovered in these analyses, as each highlights a fundamental difference between the list-learning paradigm and naturalistic memory paradigms like the one employed in the present study. The most noticeable departure from hallmark free recall dynamics in these findings is the apparent lack of a serial position effect in Figure 3C, which instead shows greater and lesser recall probabilities for events distributed across the episode. Stimuli in free recall experiments most often comprise lists of simple, common words, presented to participants in a random order. (In fact, numerous word pools have been developed based on these criteria; e.g., Friendly et al., 1982). These stimulus qualities enable two assumptions that are central to word list analyses, but frequently do not hold for real-world experiences. First, researchers conducting list-learning studies may assume that the content at each presentation index is essentially equal, and does not possess attributes that would render it, on average, more or less memorable than others. Such is rarely the case with real-world experiences or experiments meant to approximate them, and the effects of both intrinsic and observer-dependent factors on stimulus memorability are well established (for review see Chun and Turk-Browne, 2007; Bylinskii et al., 2015; Tyng et al., 2017). Second, the random ordering of list items ensures that (across participants, on average) there is no relationship between the thematic similarity of individual stimuli and their presentation positions—in other words, two successively presented items are no more likely to be highly semantically similar than they are to be highly dissimilar. In most cases, the exact opposite is true of real-world episodes. Our internal thoughts, our actions, and the physical state of the world around us all tend to follow a direct (often causal) progression. As a result, each moment of our experience tends to be inherently more similar to surrounding moments than to those in the distant past or future. Memory literature has termed this strong temporal autocorrelation “context,” and in various media that depict real-world events (e.g., movies or written stories), we recognize it as a *narrative structure*. While a random word list (by definition) has no such structure, the logical progression between ideas and actions in a naturalistic stimulus prompts the rememberer to recount presented events in order, starting with the beginning. This tendency is

490 reflected in our findings' second departure from typical free recall dynamics: a lack of increased  
491 probability of first recall for end-of-sequence events (Fig. 3A).

492 Because they disregard presentation order-dependent variability in the stimulus content, analyses  
493 such as those in Figure 3 enable a more sensitive analysis of presentation order-dependent  
494 temporal dynamics in free recall. Yet by the same token, they paint a wholly incomplete picture of  
495 memory for naturalistic episodes. In an attempt to address this shortcoming, we have developed a  
496 framework in the present study that characterizes the explicit semantic content of the stimulus and  
497 subsequent recalls. However, sensitivity to stimulus and recall content introduces a new challenge:  
498 distinguishing between levels of recall quality for a stimulus (e.g., an event) that is considered to  
499 have been "remembered." When modeling memory in an experimental setting, recall quality for  
500 individual events is often cast as binary (e.g., a given list item was simply either remembered or  
501 not remembered). Various models of memory (e.g., Yonelinas, 2002) attempt to improve upon this  
502 by including confidence ratings, rendering this binary judgement instead categorical. To better  
503 evaluate naturalistic memory quality, we introduce a continuous metric (*precision*), which reflects  
504 the level of completeness of a participant's recall for a feature-rich experience. Additionally, recall  
505 quality for a single event is typically assessed independently from that for all other events (e.g., it  
506 is difficult to "compare" a participant's binary recall success for list item 1 to that of list item 10).  
507 The second novel metric we introduce (*distinctiveness*) is based on analyzing of the correlational  
508 structure of an individual's full set of recall events, and reflects the specificity of their memory  
509 for a single experienced event. We find that both of these metrics relate to the overall number of  
510 episode events participants successfully recalled, and that our precision metric additionally relates  
511 to Chen et al. (2017)'s hand-annotated memory scores.

512 We did not find evidence that participants' average recall distinctiveness was related to their  
513 hand-annotated memory scores computed by Chen et al. (2017). One possible explanation is that,  
514 in hand-scoring each participant's verbal recall for each of 50 (manually-delimited) scenes, "[a]  
515 scene was counted as recalled if the participant described any part of the scene" (Chen et al.,  
516 2017). In other words, both an extensive description of a scene's content and a brief mention of  
517 some subset of its content were (binarily) considered equally successful recalls. By contrast, we

518 identify the event structure in participants' recalls in an unsupervised manner, independent of the  
519 episode event-timeseries, prior to mapping between episode and recall content. Our HMM-based  
520 event-segmentation produces boundaries between timepoints where the topic proportions shift in  
521 a substantial way, and because a small handful of words is unlikely to contribute significantly to  
522 the topic proportions for any sliding window, such brief scene descriptions will most often not  
523 result in a sufficiently large shift in the resulting topic proportions for the HMM to identify an  
524 event boundary. Instead, they will be grouped with a neighboring event, consequently lowering  
525 that event's distinctiveness score and by extension, the participant's overall distinctiveness score.  
526 This is in essence the qualitative difference between distinctive and indistinctive recall, and reflects  
527 the comparison shown in Figure 6C. Intriguingly, prior studies show that pattern separation, or the  
528 ability to cleanly discriminate between similar experiences, is impaired in many cognitive disorders  
529 as well as natural aging (Stark et al., 2010; Yassa et al., 2011; Yassa and Stark, 2011). Future work  
530 might explore whether and how these metrics compare between cognitively impoverished groups  
531 and healthy controls.

532 In the analyses outlined in Figure 9, we identified two networks of brain regions whose re-  
533 sponses during episode viewing were consistent with the temporal structure of the episode and  
534 recall topic trajectories, respectively. The network identified by the episode trajectory analysis in-  
535 cluded the ventromedial prefrontal cortex, left anterior temporal lobe, superior parietal and dorsal  
536 anterior cingulate cortex. The network from the episode-recall trajectory analysis also included  
537 the ventromedial prefrontal and superior parietal cortices, in addition to the posterior medial cor-  
538 tex (PMC) and the inferior temporal regions. Notably, Chen et al. (2017) also observed the PMC  
539 in a number of analyses including one that searched for regions whose activity patterns during  
540 encoding were reinstated during free recall. The PMC has been consistently identified in stud-  
541 ies involving stimuli with meaningfully structured events (Cohn-Sheely and Ranganath, 2017).  
542 Further, the PMC is part of the "posterior medial" system, a network of brain regions thought to  
543 represent situation models (Zacks et al., 2007) in support of memory, spatial navigation and social  
544 cognition (Ranganath and Ritchey, 2012). Given that we constructed our episode-recall searchlight  
545 model to capture temporal structure in the episode's semantic content (and how one's later recall

546 aligns with that structure), we speculate that the PMC may play a role in constructing mnemonic  
547 events from meaningfully structured experiences.

548 Decoding the associated significance maps with Neurosynth revealed two intriguing results.  
549 First, the top 10 terms returned for the episode-driven searchlight significance map were centered  
550 around themes of language and semantic meaning (Fig. 10A). In other words, the voxels identified  
551 as more reflective of the episode content's temporal structure (i.e., voxels with lower permutation  
552 correction-derived  $p$ -values), as defined by our model, were most likely to be reported as active in  
553 studies focused on the the neural underpinnings of semantic processing. This finding is interesting,  
554 as our model specifically captures the temporal structure of the episode's *semantic* content (e.g.,  
555 as opposed to that of the visual, auditory, or affective content). This suggests that the network of  
556 structures displayed in Figure 9C may play a roll in processing the evolving semantic content of  
557 ongoing experiences.

558 Our second searchlight analysis identified a partially overlapping network of regions (Fig. 9D)  
559 whose patterns of activity as participants viewed the episode reflected the idiosyncratic structure  
560 of each individual's later recalls. The associated significance map yielded a set of Neurosynth terms  
561 that primarily reflected names of specific structural regions (such as "thalamus," "anterior insula,"  
562 "anterior cingulate" and "inferior frontal"; Fig. 10B). Interestingly, these regions share membership  
563 in a common, large-scale functional network (termed the "salience network") involved in detect-  
564 ing and processing affective cues. In particular, the latter three regions have been implicated in  
565 functions relevant to assigning personal meaning to an experience, including: ascribing subjective  
566 value to raw, sensory input (Medford and Critchley, 2010); modulating semantic and phonological  
567 processing in response to personally salient stimuli (Kelly et al., 2007); and directing and reallo-  
568 cating attention and working memory resources towards the most relevant stimuli (Menon and  
569 Uddin, 2010). This suggests that the network of structures displayed in Figure 9D may be play a roll  
570 in transforming and restructuring ongoing experiences through the lens of one's prior experience  
571 and subjective emotions as they are encoded in memory.

572 Our work has broad implications for how we characterize and assess memory in real-world  
573 settings, such as the classroom or physician's office. For example, the most commonly used

574 classroom evaluation tools involve simply computing the proportion of correctly answered exam  
575 questions. Our work indicates that this approach is only loosely related to what educators might  
576 really want to measure: how well did the students understand the key ideas presented in the  
577 course? Under this typical framework of assessment, the same exam score of 50% could be  
578 ascribed to two very different students: one who attended the full course but struggled to learn  
579 more than a broad overview of the material, and one who attended only half of the course but  
580 understood the material perfectly. Instead, one could apply our computational framework to build  
581 explicit content models of the course material and exam questions. This approach would provide  
582 a more nuanced and specific view into which aspects of the material students had learned well  
583 (or poorly). In clinical settings, memory measures that incorporate such explicit content models  
584 might also provide more direct evaluations of patients' memories.

## 585 Methods

### 586 Experimental design and data collection

587 Data were collected by Chen et al. (2017). In brief, participants ( $n = 22$ ) viewed the first 48 minutes  
588 of "A Study in Pink", the first episode of the BBC television series *Sherlock*, while fMRI volumes  
589 were collected (TR = 1500 ms). Participants were pre-screened to ensure they had never seen any  
590 episode of the show before. The stimulus was divided into a 23 min (946 TR) and a 25 min (1030 TR)  
591 segment to mitigate technical issues related to the scanner. After finishing the clip, participants  
592 were instructed to (quoting from Chen et al., 2017) "describe what they recalled of the [episode]  
593 in as much detail as they could, to try to recount events in the original order they were viewed  
594 in, and to speak for at least 10 minutes if possible but that longer was better. They were told that  
595 completeness and detail were more important than temporal order, and that if at any point they  
596 realized they had missed something, to return to it. Participants were then allowed to speak for  
597 as long as they wished, and verbally indicated when they were finished (e.g., 'I'm done')." Five  
598 participants were dropped from the original dataset due to excessive head motion (2 participants),

599 insufficient recall length (2 participants), or falling asleep during stimulus viewing (1 participant),  
600 resulting in a final sample size of  $n = 17$ . For additional details about the experimental procedure  
601 and scanning parameters, see Chen et al. (2017). The experimental protocol was approved by  
602 Princeton University's Institutional Review Board.

603 After preprocessing the fMRI data and warping the images into a standard (3 mm<sup>3</sup> MNI) space,  
604 the voxel activations were z-scored (within voxel) and spatially smoothed using a 6 mm (full width  
605 at half maximum) Gaussian kernel. The fMRI data were also cropped so that all episode-viewing  
606 data were aligned across participants. This included a constant 3 TR (4.5 s) shift to account for the  
607 lag in the hemodynamic response. (All of these preprocessing steps followed Chen et al., 2017,  
608 where additional details may be found.)

609 The video stimulus was divided into 1,000 fine-grained “scenes” and annotated by an inde-  
610 pendent coder. For each of these 1,000 scenes, the following information was recorded: a brief  
611 narrative description of what was happening, the location where the scene took place, whether  
612 that location was indoors or outdoors, the names of all characters on-screen, the name(s) of the  
613 character(s) in focus in the shot, the name(s) of the character(s) currently speaking, the camera  
614 angle of the shot, a transcription of any text appearing on-screen, and whether or not there was  
615 music present in the background. Each scene was also tagged with its onset and offset time, in  
616 both seconds and TRs.

## 617 **Data and code availability**

618 The fMRI data we analyzed are available online [here](#). The behavioral data and all of our analysis  
619 code may be downloaded [here](#).

## 620 **Statistics**

621 All statistical tests performed in the behavioral analyses were two-sided. All statistical tests per-  
622 formed in the neural data analyses were two-sided, except for the permutation-based thresholding,  
623 which was one-sided. In this case, we were specifically interested in identifying voxels whose acti-

624 vation time series reflected the temporal structure of the episode and recall trajectories to a *greater*  
625 extent than that of the phase-shifted trajectories.

## 626 **Modeling the dynamic content of the episode and recall transcripts**

### 627 **Topic modeling**

628 The input to the topic model we trained to characterize the dynamic content of the episode  
629 comprised 998 hand-generated annotations of short (mean: 2.96s) scenes spanning the video  
630 clip (Chen et al., 2017 generated 1000 annotations total; we removed two annotations referring to  
631 a break between the first and second scan sessions, during which no fMRI data was collected).  
632 We concatenated the text for all of the annotated features within each segment, creating a “bag of  
633 words” describing each scene and performed some minor preprocessing (e.g., stemming possessive  
634 nouns and removing punctuation). We then re-organized the text descriptions into overlapping  
635 sliding windows spanning (up to) 50 scenes each. In other words, we estimated the “context”  
636 for each scene using the text descriptions of the preceding 25 scenes, the present scene, and the  
637 following 24 scenes. To model the context for scenes near the beginning of the episode (i.e., within  
638 25 scenes of the beginning or end), we created overlapping sliding windows that grew in size  
639 from one scene to the full length. We also tapered the sliding window lengths at the end of the  
640 episode, whereby scenes within fewer than 24 scenes of the end of the episode were assigned  
641 sliding windows that extended to the end of the episode. This procedure ensured that each scene’s  
642 content was represented in the text corpus an equal number of times.

643 We trained our model using these overlapping text samples with `scikit-learn` (version 0.19.1;  
644 Pedregosa et al., 2011), called from our high-dimensional visualization and text analysis software,  
645 `HyperTools` (Heusser et al., 2018b). Specifically, we used the `CountVectorizer` class to transform  
646 the text from each window into a vector of word counts (using the union of all words across all  
647 scenes as the “vocabulary,” excluding English stop words); this yielded a number-of-windows  
648 by number-of-words *word count* matrix. We then used the `LatentDirichletAllocation` class  
649 (`topics=100`, `method='batch'`) to fit a topic model (Blei et al., 2003) to the word count matrix,

yielding a number-of-windows (1047) by number-of-topics (100) *topic proportions* matrix. The topic proportions matrix describes the gradually evolving mix of topics (latent themes) present in each scene. Next, we transformed the topic proportions matrix to match the 1976 fMRI volume acquisition times. We assigned each topic vector to the timepoint (in seconds) midway between the beginning of the first scene and the end of the last scene in its corresponding sliding text window. By doing so, we warped the linear temporal distance between consecutive topic vectors to align with the inconsistent temporal distance between consecutive annotations (whose durations varied greatly). We then rescaled these timepoints to 1.5s TR units, and used linear interpolation to estimate a topic vector for each TR. This resulted in a number-of-TRs (1976) by number-of-topics (100) matrix.

We created similar topic proportions matrices using hand-annotated transcripts of each participant's verbal recall of the episode (annotated by Chen et al., 2017). We tokenized the transcript into a list of sentences, and then re-organized the list into overlapping sliding windows spanning (up to) 10 sentences each, analogously to how we parsed the episode annotations. In turn, we transformed each window's sentences into a word count vector (using the same vocabulary as for the episode model), and then we used the topic model already trained on the episode scenes to compute the most probable topic proportions for each sliding window. This yielded a number-of-windows (range: 83–312) by number-of-topics (100) topic proportions matrix for each participant. These reflected the dynamic content of each participant's recalls. Note: for details on how we selected the episode and recall window lengths and number of topics, see *Supporting Information* and Figure S1.

#### 671 **Parsing topic trajectories into events using Hidden Markov Models**

We parsed the topic trajectories of the episode and participants' recalls into events using Hidden Markov Models (HMMs; Rabiner, 1989). Given the topic proportions matrix (describing the mix of topics at each timepoint) and a number of states,  $K$ , an HMM recovers the set of state transitions that segments the timeseries into  $K$  discrete states. Following Baldassano et al. (2017), we imposed an additional set of constraints on the discovered state transitions that ensured that each state was

677 encountered exactly once (i.e., never repeated). We used the BrainIAK toolbox (Capota et al., 2017)  
678 to implement this segmentation.

679 We used an optimization procedure to select the appropriate  $K$  for each topic proportions  
680 matrix. Prior studies on narrative structure and processing have shown that we both perceive  
681 and internally represent the world around us at multiple, hierarchical timescales (e.g., Hasson  
682 et al., 2008; Lerner et al., 2011; Hasson et al., 2015; Chen et al., 2017; Baldassano et al., 2017, 2018).  
683 However, for the purposes of our framework, we sought to identify the single timeseries of event-  
684 representations that is emphasized *most heavily* in the temporal structure of the episode and of each  
685 participant's recall. We quantified this as the set of  $K$  states that maximized the similarity between  
686 topic vectors for timepoints comprising each state, while minimizing the similarity between topic  
687 vectors for timepoints across different states. Specifically, we computed (for each matrix)

$$\operatorname{argmax}_K [W_1(a, b)],$$

688 where  $a$  was the distribution of within-state topic vector correlations, and  $b$  was the distribution of  
689 across-state topic vector correlations . We computed the first Wasserstein distance ( $W_1$ ; also known  
690 as *Earth mover's distance*; Dobrushin, 1970; Ramdas et al., 2017) between these distributions for a  
691 large range of possible  $K$ -values (range [2, 50]), and selected the  $K$  that yielded the maximum value.  
692 Figure 2B displays the event boundaries returned for the episode, and Figure S4 displays the event  
693 boundaries returned for each participant's recalls. See Figure S6 for the optimization functions  
694 for the episode and recalls. After obtaining these event boundaries, we created stable estimates  
695 of the content represented in each event by averaging the topic vectors across timepoints between  
696 each pair of event boundaries. This yielded a number-of-events by number-of-topics matrix for  
697 the episode and recalls from each participant.

698 **Naturalistic extensions of classic list-learning analyses**

699 In traditional list-learning experiments, participants view a list of items (e.g., words) and then  
700 recall the items later. Our episode-recall event matching approach affords us the ability to analyze

701 memory in a similar way. The episode and recall events can be treated analogously to studied and  
702 recalled “items” in a list-learning study. We can then extend classic analyses of memory perfor-  
703 mance and dynamics (originally designed for list-learning experiments) to the more naturalistic  
704 episode recall task used in this study.

705 Perhaps the simplest and most widely used measure of memory performance is *accuracy*—i.e.,  
706 the proportion of studied (experienced) items (in this case, episode events) that the participant later  
707 remembered. Chen et al. (2017) used this method to rate each participant’s memory quality by  
708 computing the proportion of (50, manually identified) scenes mentioned in their recall. We found a  
709 strong across-participants correlation between these independent ratings and the proportion of 30  
710 HMM-identified episode events matched to participants’ recalls (Pearson’s  $r(15) = 0.71, p = 0.002$ ).  
711 We further considered a number of more nuanced memory performance measures that are typically  
712 associated with list-learning studies. We also provide a software package, Quail, for carrying out  
713 these analyses (Heusser et al., 2017).

714 **Probability of first recall (PFR).** PFR curves (Welch and Burnett, 1924; Postman and Phillips,  
715 1965; Atkinson and Shiffrin, 1968) reflect the probability that an item will be recalled first as a  
716 function of its serial position during encoding. To carry out this analysis, we initialized a number-  
717 of-participants (17) by number-of-episode-events (30) matrix of zeros. Then for each participant,  
718 we found the index of the episode event that was recalled first (i.e., the episode event whose topic  
719 vector was most strongly correlated with that of the first recall event) and filled in that index in  
720 the matrix with a 1. Finally, we averaged over the rows of the matrix, resulting in a 1 by 30 array  
721 representing the proportion of participants that recalled an event first, as a function of the order of  
722 the event’s appearance in the episode (Fig. 3A).

723 **Lag conditional probability curve (lag-CRP).** The lag-CRP curve (Kahana, 1996) reflects the  
724 probability of recalling a given item after the just-recalled item, as a function of their relative  
725 encoding positions (or *lag*). In other words, a lag of 1 indicates that a recalled item was presented  
726 immediately after the previously recalled item, and a lag of -3 indicates that a recalled item came 3

727 items before the previously recalled item. For each recall transition (following the first recall), we  
728 computed the lag between the current recall event and the next recall event, normalizing by the  
729 total number of possible transitions. This yielded a number-of-participants (17) by number-of-lags  
730 (-29 to +29; 58 lags total excluding lags of 0) matrix. We averaged over the rows of this matrix to  
731 obtain a group-averaged lag-CRP curve (Fig. 3B).

732 **Serial position curve (SPC).** SPCs (Murdock, 1962) reflect the proportion of participants that  
733 remember each item as a function of the items' serial positions during encoding. We initialized  
734 a number-of-participants (17) by number-of-episode-events (30) matrix of zeros. Then, for each  
735 recalled event, for each participant, we found the index of the episode event that the recalled  
736 event most closely matched (via the correlation between the events' topic vectors) and entered a  
737 1 into that position in the matrix. This resulted in a matrix whose entries indicated whether or  
738 not each event was recalled by each participant (depending on whether the corresponding entires  
739 were set to one or zero). Finally, we averaged over the rows of the matrix to yield a 1 by 30 array  
740 representing the proportion of participants that recalled each event as a function of the events'  
741 order appearance in the episode (Fig. 3C).

742 **Temporal clustering scores.** Temporal clustering describes a participant's tendency to organize  
743 their recall sequences by the learned items' encoding positions. For instance, if a participant  
744 recalled the episode events in the exact order they occurred (or in exact reverse order), this would  
745 yield a score of 1. If a participant recalled the events in random order, this would yield an expected  
746 score of 0.5. For each recall event transition (and separately for each participant), we sorted all  
747 not-yet-recalled events according to their absolute lag (i.e., distance away in the episode). We  
748 then computed the percentile rank of the next event the participant recalled. We averaged these  
749 percentile ranks across all of the participant's recalls to obtain a single temporal clustering score  
750 for the participant.

751 **Semantic clustering scores.** Semantic clustering describes a participant's tendency to recall se-  
752 mantically similar presented items together in their recall sequences. Here, we used the topic

vectors for each event as a proxy for its semantic content. Thus, the similarity between the semantic content for two events can be computed by correlating their respective topic vectors. For each recall event transition, we sorted all not-yet-recalled events according to how correlated the topic vector of the closest-matching episode event was to the topic vector of the closest-matching episode event to the just-recalled event. We then computed the percentile rank of the observed next recall. We averaged these percentile ranks across all of the participant's recalls to obtain a single semantic clustering score for the participant.

## Novel naturalistic memory metrics

**Precision.** We tested whether participants who recalled more events were also more *precise* in their recollections. For each participant, we computed the average correlation between the topic vectors for each recall event and those of its closest-matching episode event. This gave a single value per participant representing the average precision across all recalled events. We then correlated these values with both hand-annotated and model-derived (i.e., the number of unique episode events matched by a participant's recall events) memory performance.

**Distinctiveness.** We also considered the *distinctiveness* of each recalled event. That is, how unique a participant's description of a episode event was, versus their descriptions of other episode events. We hypothesized that participants with high memory performance might describe each event in a more distinctive way (relative to those with lower memory performance who might describe events in a more general way). To test this hypothesis we define a distinctiveness score for each recall event  $i$  as

$$d(i) = 1 - \frac{1}{N-1} \sum_{j=i} \text{corr}(\text{event}_i, \text{event}_j)$$

where the average is taken over the correlation between the recall event  $i$ 's topic vector and the topic vectors from all other recall events from that participant. We averaged these distinctiveness scores across all of the events recalled by the given participant to get the participant's distinctiveness

776 score. We correlated these distinctiveness scores with hand-annotated and model-derived memory  
777 performance scores across-subjects, as above.

778 **Averaging correlations** In all instances where we performed statistical tests involving precision  
779 or distinctiveness scores, we used the Fisher  $z$ -transformation (Fisher, 1925) to stabilize the variance  
780 across the distribution of correlation values prior to performing the test. Similarly, when averaging  
781 precision or distinctiveness scores, we  $z$ -transformed the scores prior to computing the mean, and  
782 inverse  $z$ -transformed the result.

783 **Visualizing the episode and recall topic trajectories**

784 We used the UMAP algorithm (McInnes et al., 2018) to project the 100-dimensional topic space onto  
785 a two-dimensional space for visualization (Figs. 7, 8). To ensure that all of the trajectories were  
786 projected onto the *same* lower dimensional space, we computed the low-dimensional embedding  
787 on a “stacked” matrix created by vertically concatenating the events-by-topics topic proportions  
788 matrices for the episode, across-participants average recall and all 17 individual participants’ re-  
789 calls. We then separated the rows of the result (a total-number-of-events by two matrix) back into  
790 individual matrices for the episode topic trajectory, across-participant average recall trajectory and  
791 the trajectories for each individual participant’s recalls (Fig. 7). This general approach for dis-  
792 covering a shared low-dimensional embedding for a collections of high-dimensional observations  
793 follows Heusser et al. (2018b).

794 We optimized the manifold space for visualization based on two criteria: First, that the 2D em-  
795 bedding of the episode trajectory should reflect its original 100-dimensional structure as faithfully  
796 as possible. Second, that the path traversed by the embedded episode trajectory should intersect  
797 itself a minimal number of times. The first criteria helps bolster the validity of visual intuitions  
798 about relationships between sections of episode content, based on their locations in the embedding  
799 space. The second criteria was motivated by the observed low off-diagonal values in the episode  
800 trajectory’s temporal correlation matrix (suggesting that the same topic-space coordinates should  
801 not be revisited; see Figure 2A in the main text). For further details on how we created this

802 low-dimensional embedding space, see *Supporting Information*.

803 **Estimating the consistency of flow through topic space across participants**

804 In Figure 7B, we present an analysis aimed at characterizing locations in topic space that dif-  
805 ferent participants move through in a consistent way (via their recall topic trajectories). The  
806 two-dimensional topic space used in our visualizations (Fig. 7) comprised a 60 x 60 (arbitrary  
807 units) square. We tiled this space with a 50 x 50 grid of evenly spaced vertices, and defined a  
808 circular area centered on each vertex whose radius was two times the distance between adjacent  
809 vertices (i.e., 2.4 units). For each vertex, we examined the set of line segments formed by connecting  
810 each pair successively recalled events, across all participants, that passed through this circle. We  
811 computed the distribution of angles formed by those segments and the  $x$ -axis, and used a Rayleigh  
812 test to determine whether the distribution of angles was reliably “peaked” (i.e., consistent across  
813 all transitions that passed through that local portion of topic space). To create Figure 7B we drew  
814 an arrow originating from each grid vertex, pointing in the direction of the average angle formed  
815 by the line segments that passed within 2.4 units. We set the arrow lengths to be inversely propor-  
816 tional to the  $p$ -values of the Rayleigh tests at each vertex. Specifically, for each vertex we converted  
817 all of the angles of segments that passed within 2.4 units to unit vectors, and we set the arrow  
818 lengths at each vertex proportional to the length of the (circular) mean vector. We also indicated  
819 any significant results ( $p < 0.05$ , corrected using the Benjamini-Hochberg procedure) by coloring  
820 the arrows in blue (darker blue denotes a lower  $p$ -value, i.e., a longer mean vector); all tests with  
821  $p \geq 0.05$  are displayed in gray and given a lower opacity value.

822 **Searchlight fMRI analyses**

823 In Figure 9, we present two analyses aimed at identifying brain regions whose responses (as partic-  
824 ipants viewed the episode) exhibited a particular temporal structure. We developed a searchlight  
825 analysis wherein we constructed a 5 x 5 x 5 cube of voxels (following Chen et al., 2017) centered  
826 on each voxel in the brain, and for each of these cubes, computed the temporal correlation matrix  
827 of the voxel responses during episode viewing. Specifically, for each of the 1976 volumes collected

828 during episode viewing, we correlated the activity patterns in the given cube with the activity  
829 patterns (in the same cube) collected during every other timepoint. This yielded a 1976 by 1976  
830 correlation matrix for each cube. Note: participant 5's scan ended 75s early, and in Chen et al.,  
831 2017's publicly released dataset, their scan data was padded to match the length of the other partic-  
832 ipants'. For our searchlight analyses, we removed this padded data (i.e., the last 50 TRs), resulting  
833 in a 1925 by 1925 correlation matrix for each cube in participant 5's brain.

834 Next, we constructed a series of "template" matrices. The first template reflected the timecourse  
835 of the episode's topic trajectory, and the others reflected the timecourse of each participant's recall  
836 trajectory. To construct the episode template, we computed the correlations between the topic  
837 proportions estimated for every pair of TRs (prior to segmenting the trajectory into discrete events;  
838 i.e., the correlation matrix shown in Figs. 2B and 9A). We constructed similar temporal correlation  
839 matrices for each participant's recall topic trajectory (Figs. 2D, S4). However, to correct for length  
840 differences and potential non-linear transformations between viewing time and recall time, we  
841 first used dynamic time warping (Berndt and Clifford, 1994) to temporally align participants'  
842 recall topic trajectories with the episode topic trajectory. An example correlation matrix before and  
843 after warping is shown in Fig. 9B. This yielded a 1976 by 1976 correlation matrix for the episode  
844 template and for each participant's recall template.

845 The temporal structure of the episode's content (as described by our model) is captured in the  
846 block-diagonal structure of the episode's temporal correlation matrix (e.g., Figs. 2B, 9A), with time  
847 periods of thematic stability represented as dark blocks of varying sizes. Inspecting the episode  
848 correlation matrix suggests that the episode's semantic content is highly temporally specific (i.e.,  
849 the correlations between topic vectors from distant timepoints are almost all near zero). By contrast,  
850 the activity patterns of individual (cubes of) voxels can encode relatively limited information on  
851 their own, and their activity frequently contributes to multiple separate functions (Freedman  
852 et al., 2001; Sigman and Dehaene, 2008; Charron and Koechlin, 2010; Rishel et al., 2013). By  
853 nature, these two attributes give rise to similarities in activity across large timescales that may not  
854 necessarily reflect a single task. To enable a more sensitive analysis of brain regions whose shifts  
855 in activity patterns mirrored shifts in the semantic content of the episode or recalls, we restricted

the temporal correlations we considered to the timescale of semantic information captured by our model. Specifically, we isolated the upper triangle of the episode correlation matrix and created a “proximal correlation mask” that included only diagonals from the upper triangle of the episode correlation matrix up to the first diagonal that contained no positive correlations. Applying this mask to the full episode correlation matrix was analogous to excluding diagonals beyond the corner of the largest diagonal block. In other words, the timescale of temporal correlations we considered corresponded to the longest period of thematic stability in the episode, and by extension the longest expected period of thematic stability in participants’ recalls and the longest period of stability we might expect to see in voxel activity arising from processing or encoding episode content. Figure 9 shows this proximal correlation mask applied to the temporal correlation matrices for the episode, an example participant’s (warped) recall, and an example cube of voxels from our searchlight analyses.

To determine which (cubes of) voxel responses matched the episode template, we correlated the proximal diagonals from the upper triangle of the voxel correlation matrix for each cube with the proximal diagonals from episode template matrix (Kriegeskorte et al., 2008). This yielded, for each participant, a voxelwise map of correlation values. We then performed a one-sample  $t$ -test on the distribution of (Fisher  $z$ -transformed) correlations at each voxel, across participants. This resulted in a value for each voxel (cube), describing how reliably its timecourse followed that of the episode.

We further sought to ensure that our analysis identified regions where the activations’ temporal structure specifically reflected that of the episode, rather than regions whose activity was simply autocorrelated at a width similar to the episode template’s diagonal. To achieve this, we used a phase shift-based permutation procedure, whereby we circularly shifted the episode’s topic trajectory by a random number of timepoints, computed the resulting “null” episode template, and re-ran the searchlight analysis, in full. (For each of the 100 permutations, the same random shift was used for all participants). We  $z$ -scored the observed (unshifted) result at each voxel against the distribution of permutation-derived “null” results, and estimated a  $p$ -value by computing the proportion of shifted results that yielded larger values. To create the map in Figure 9C, we

884 thresholded out any voxels whose similarity to the unshifted episode's structure fell below the 95<sup>th</sup>  
885 percentile of the permutation-derived similarity results.

886 We used an analogous procedure to identify which voxels' responses reflected the recall tem-  
887 plates. For each participant, we correlated the proximal diagonals from the upper triangle of the  
888 correlation matrix for each cube of voxels with the proximal diagonals from the upper triangle of  
889 their (time-warped) recall correlation matrix. As in the episode template analysis, this yielded a  
890 voxelwise map of correlation coefficients per participant. However, whereas the episode analysis  
891 compared every participant's responses to the same template, here the recall templates were unique  
892 for each participant. As in the analysis described above, we *t*-scored the (Fisher *z*-transformed)  
893 voxelwise correlations, and used the same permutation procedure we developed for the episode  
894 responses to ensure specificity to the recall timeseries and assign significance values. To create the  
895 map in Figure 9D we again thresholded out any voxels whose scores were below the 95<sup>th</sup> percentile  
896 of the permutation-derived null distribution.

## 897 **Neurosynth decoding analyses**

898 Neurosynth parses a massive online database of over 14,000 neuroimaging studies and constructs  
899 meta-analysis images for over 13,000 psychology- and neuroscience-related terms, based on NIfTI  
900 images accompanying studies where those terms appear at a high frequency. Given a novel image  
901 (tagged with its value type; e.g., *t*-, *F*- or *p*-statistics), Neurosynth returns a list of terms whose  
902 meta-analysis images are most similar. Our permutation procedure yielded, for each of the two  
903 searchlight analyses, a voxelwise map of significance (*p*-statistic) values. These maps describe the  
904 extent to which each voxel *specifically* reflected the temporal structure of the episode or individuals'  
905 recalls (i.e., for each voxel, the proportion of phase-shifted topic vector correlation matrices less  
906 similar to the voxel activity correlation matrix than the unshifted episode's correlation matrix).  
907 We inputted the two statistical maps described above to Neurosynth to create a list of the 10 most  
908 representative terms for each map.

909 **References**

- 910 Atkinson, R. C. and Shiffrin, R. M. (1968). Human memory: A proposed system and its control  
911 processes. In Spence, K. W. and Spence, J. T., editors, *The psychology of learning and motivation*,  
912 volume 2, pages 89–105. Academic Press, New York.
- 913 Baldassano, C., Chen, J., Zadbood, A., Pillow, J. W., Hasson, U., and Norman, K. A. (2017).  
914 Discovering event structure in continuous narrative perception and memory. *Neuron*, 95(3):709–  
915 721.
- 916 Baldassano, C., Hasson, U., and Norman, K. A. (2018). Representation of real-world event schemas  
917 during narrative perception. *Journal of Neuroscience*, 38(45):9689–9699.
- 918 Berndt, D. J. and Clifford, J. (1994). Using dynamic time warping to find patterns in time series. In  
919 *KDD workshop*, volume 10, pages 359–370.
- 920 Blei, D. M. and Lafferty, J. D. (2006). Dynamic topic models. In *Proceedings of the 23rd International  
921 Conference on Machine Learning*, ICML '06, pages 113–120, New York, NY, US. ACM.
- 922 Blei, D. M., Ng, A. Y., and Jordan, M. I. (2003). Latent dirichlet allocation. *Journal of Machine  
923 Learning Research*, 3:993 – 1022.
- 924 Brown, T. B., Mann, B., Ryder, N., Subbiah, M., Kaplan, J., Dhariwal, P., Neelakantan, A., Shyam,  
925 P., Sastry, G., Askell, A., Agarwal, S., Herbert-Voss, A., Krueger, G., Henighan, T., Child, R.,  
926 Ramesh, A., Ziegler, D. M., Wu, J., Winter, C., Hesse, C., Chen, M., Sigler, E., Litwin, M., Gray, S.,  
927 Chess, B., Clark, J., Berner, C., McCandlish, S., Radford, A., Sutskever, I., and Amodei, D. (2020).  
928 Language models are few-shot learners. *arXiv*, 2005.14165.
- 929 Brunec, I. K., Moscovitch, M. M., and Barene, M. D. (2018). Boundaries shape cognitive represen-  
930 tations of spaces and events. *Trends in Cognitive Sciences*, 22(7):637–650.
- 931 Bylinskii, Z., Isola, P., Bainbridge, C., Torralba, A., and Oliva, A. (2015). Intrinsic and extrinsic  
932 effects on image memorability. *Vision Research*, 116:165–178.

- 933 Capota, M., Turek, J., Chen, P.-H., Zhu, X., Manning, J. R., Sundaram, N., Keller, B., Wang, Y., and  
934 Shin, Y. S. (2017). Brain imaging analysis kit.
- 935 Cer, D., Yang, Y., Kong, S. Y., Hua, N., Limtiaco, N., John, R. S., Constant, N., Guajardo-Cespedes,  
936 M., Yuan, S., Tar, C., Sung, Y.-H., Strope, B., and Kurzweil, R. (2018). Universal sentence encoder.  
937 *arXiv*, 1803.11175.
- 938 Charron, S. and Koechlin, E. (2010). Divided representations of current goals in the human frontal  
939 lobes. *Science*, 328(5976):360–363.
- 940 Chen, J., Leong, Y. C., Honey, C. J., Yong, C. H., Norman, K. A., and Hasson, U. (2017). Shared  
941 memories reveal shared structure in neural activity across individuals. *Nature Neuroscience*,  
942 20(1):115.
- 943 Chun, M. and Turk-Browne, N. (2007). Interactions between attention and memory. *Current opinion  
944 in neurobiology*, 17(2):177–184.
- 945 Clewett, D. and Davachi, L. (2017). The ebb and flow of experience determines the temporal  
946 structure of memory. *Curr Opin Behav Sci*, 17:186–193.
- 947 Cohn-Sheely, B. I. and Ranganath, C. (2017). Time regained: how the human brain constructs  
948 memory for time. *Current Opinion in Behavioral Sciences*, 17:169–177.
- 949 Dobrushin, R. L. (1970). Prescribing a system of random variables by conditional distributions.  
950 *Theory of Probability & Its Applications*, 15(3):458–486.
- 951 DuBrow, S. and Davachi, L. (2013). The influence of contextual boundaries on memory for the  
952 sequential order of events. *Journal of Experimental Psychology: General*, 142(4):1277–1286.
- 953 Ezzyat, Y. and Davachi, L. (2011). What constitutes an episode in episodic memory? *Psychological  
954 Science*, 22(2):243–252.
- 955 Fisher, R. A. (1925). *Statistical Methods for Research Workers*. Oliver and Boyd.

- 956 Freedman, D., Riesenhuber, M., Poggio, T., and Miller, E. (2001). Categorical representation of  
957 visual stimuli in the primate prefrontal cortex. *Science*, 291(5502):312–316.
- 958 Friendly, M., Franklin, P. E., Hoffman, D., and Rubin, D. C. (1982). The Toronto Word Pool:  
959 Norms for imagery, concreteness, orthographic variables, and grammatical usage for 1,080  
960 words. *Behavior Research Methods and Instrumentation*, 14:375–399.
- 961 Hasson, U., Chen, J., and Honey, C. J. (2015). Hierarchical process memory: memory as an integral  
962 component of information processing. *Trends in Cognitive Science*, 19(6):304–315.
- 963 Hasson, U., Yang, E., Vallines, I., Heeger, D. J., and Rubin, N. (2008). A hierarchy of temporal  
964 receptive windows in human cortex. *Journal of Neuroscience*, 28(10):2539–2550.
- 965 Heusser, A. C., Ezzyat, Y., Shiff, I., and Davachi, L. (2018a). Perceptual boundaries cause mnemonic  
966 trade-offs between local boundary processing and across-trial associative binding. *Journal of*  
967 *Experimental Psychology Learning, Memory, and Cognition*, 44(7):1075–1090.
- 968 Heusser, A. C., Fitzpatrick, P. C., Field, C. E., Ziman, K., and Manning, J. R. (2017). Quail: a  
969 Python toolbox for analyzing and plotting free recall data. *The Journal of Open Source Software*,  
970 10.21105/joss.00424.
- 971 Heusser, A. C., Ziman, K., Owen, L. L. W., and Manning, J. R. (2018b). HyperTools: a Python  
972 toolbox for gaining geometric insights into high-dimensional data. *Journal of Machine Learning*  
973 *Research*, 18(152):1–6.
- 974 Howard, M. W. and Kahana, M. J. (2002). A distributed representation of temporal context. *Journal*  
975 *of Mathematical Psychology*, 46:269–299.
- 976 Howard, M. W., MacDonald, C. J., Tiganj, Z., Shankar, K. H., Du, Q., Hasselmo, M. E., and H., E.  
977 (2014). A unified mathematical framework for coding time, space, and sequences in the medial  
978 temporal lobe. *Journal of Neuroscience*, 34(13):4692–4707.
- 979 Howard, M. W., Viskontas, I. V., Shankar, K. H., and Fried, I. (2012). Ensembles of human MTL  
980 neurons “jump back in time” in response to a repeated stimulus. *Hippocampus*, 22:1833–1847.

- 981 Huk, A., Bonnen, K., and He, B. J. (2018). Beyond trial-based paradigms: continuous behavior, on-  
982 going neural activity, and naturalistic stimuli. *Journal of Neuroscience*, 10.1523/JNEUROSCI.1920-  
983 17.2018.
- 984 Kahana, M. J. (1996). Associative retrieval processes in free recall. *Memory & Cognition*, 24:103–109.
- 985 Kelly, S., Lloyd, D., Nurmikko, T., and Roberts, N. (2007). Retrieving autobiographical memories  
986 of painful events activates the anterior cingulate cortex and inferior frontal gyrus. *The Journal of  
987 Pain*, 8(4):307–314.
- 988 Kriat, A. and Goldsmith, M. (1994). Memory in naturalistic and laboratory contexts: distin-  
989 guishing accuracy-oriented and quantity-oriented approaches to memory assessment. *Journal of  
990 Experimental Psychology: General*, 123(3):297–315.
- 991 Kriegeskorte, N., Mur, M., and Bandettini, P. (2008). Representational similarity analysis – con-  
992 nnecting the branches of systems neuroscience. *Frontiers in Systems Neuroscience*, 2:1 – 28.
- 993 Landauer, T. K. and Dumais, S. T. (1997). A solution to Plato’s problem: the latent semantic  
994 analysis theory of acquisition, induction, and representation of knowledge. *Psychological Review*,  
995 104:211–240.
- 996 Lerner, Y., Honey, C. J., Silbert, L. J., and Hasson, U. (2011). Topographic mapping of a hierarchy  
997 of temporal receptive windows using a narrated story. *Journal of Neuroscience*, 31(8):2906–2915.
- 998 Manning, J. R. (2019). Episodic memory: mental time travel or a quantum ‘memory wave’ function?  
999 *PsyArXiv*, doi:10.31234/osf.io/6zjwb.
- 1000 Manning, J. R. (2020). Context reinstatement. In Kahana, M. J. and Wagner, A. D., editors, *Handbook  
1001 of Human Memory*. Oxford University Press.
- 1002 Manning, J. R., Norman, K. A., and Kahana, M. J. (2015). The role of context in episodic memory.  
1003 In Gazzaniga, M., editor, *The Cognitive Neurosciences, Fifth edition*, pages 557–566. MIT Press.

- 1004 Manning, J. R., Polyn, S. M., Baltuch, G., Litt, B., and Kahana, M. J. (2011). Oscillatory patterns  
1005 in temporal lobe reveal context reinstatement during memory search. *Proceedings of the National*  
1006 *Academy of Sciences, USA*, 108(31):12893–12897.
- 1007 McInnes, L., Healy, J., and Melville, J. (2018). UMAP: Uniform manifold approximation and  
1008 projection for dimension reduction. *arXiv*, 1802(03426).
- 1009 Medford, N. and Critchley, H. D. (2010). Conjoint activity of anterior insular and anterior cingulate  
1010 cortex: awareness and response. *Brain Structure and Function*, 214(5-6):535–549.
- 1011 Menon, V. and Uddin, L. Q. (2010). Saliency, switching, attention and control: a network model of  
1012 insula function. *Brain Structure and Function*, 214(5-6):655–667.
- 1013 Mikolov, T., Chen, K., Corrado, G., and Dean, J. (2013). Efficient estimation of word representations  
1014 in vector space. *arXiv*, 1301.3781.
- 1015 Mueller, A., Fillion-Robin, J.-C., Boidol, R., Tian, F., Nechifor, P., yoonsubKim, Peter, Rampin, R.,  
1016 Corvellec, M., Medina, J., Dai, Y., Petrushev, B., Langner, K. M., Hong, Alessio, Ozsvald, I.,  
1017 vkolmakov, Jones, T., Bailey, E., Rho, V., IgorAPM, Roy, D., May, C., foobuzz, Piyush, Seong,  
1018 L. K., Goey, J. V., Smith, J. S., Gus, and Mai, F. (2018). WordCloud 1.5.0: a little word cloud  
1019 generator in Python. *Zenodo*, <https://zenodo.org/record/1322068#.W4tPKZNKh24>.
- 1020 Murdock, B. B. (1962). The serial position effect of free recall. *Journal of Experimental Psychology*,  
1021 64:482–488.
- 1022 Paller, K. A. and Wagner, A. D. (2002). Observing the transformation of experience into memory.  
1023 *Trends in Cognitive Sciences*, 6(2):93–102.
- 1024 Pedregosa, F., Varoquaux, G., Gramfort, A., Michel, V., Thirion, B., Grisel, O., Blondel, M., Pretten-  
1025 hofer, P., Weiss, R., Dubourg, V., Vanderplas, J., Passos, A., Cournapeau, D., Brucher, M., Perrot,  
1026 M., and Duchesnay, E. (2011). Scikit-learn: Machine learning in Python. *Journal of Machine*  
1027 *Learning Research*, 12:2825–2830.

- 1028 Polyn, S. M., Norman, K. A., and Kahana, M. J. (2009). A context maintenance and retrieval model  
1029 of organizational processes in free recall. *Psychological Review*, 116(1):129–156.
- 1030 Postman, L. and Phillips, L. W. (1965). Short-term temporal changes in free recall. *Quarterly Journal*  
1031 *of Experimental Psychology*, 17:132–138.
- 1032 Rabiner, L. (1989). A tutorial on Hidden Markov Models and selected applications in speech  
1033 recognition. *Proceedings of the IEEE*, 77(2):257–286.
- 1034 Radford, A., Wu, J., Child, R., Luan, D., Amodei, D., and Sutskever, I. (2019). Language models are  
1035 unsupervised multitask learners. *OpenAI Blog*, 1(8).
- 1036 Radvansky, G. A. and Zacks, J. M. (2017). Event boundaries in memory and cognition. *Curr Opin*  
1037 *Behav Sci*, 17:133–140.
- 1038 Ramdas, A., Trillos, N., and Cuturi, M. (2017). On wasserstein two-sample testing and related  
1039 families of nonparametric tests. *Entropy*, 19(2):47.
- 1040 Ranganath, C. and Ritchey, M. (2012). Two cortical systems for memory-guided behavior. *Nature*  
1041 *Reviews Neuroscience*, 13:713 – 726.
- 1042 Rishel, C. A., Huang, G., and Freedman, D. J. (2013). Independent category and spatial encoding  
1043 in parietal cortex. *Neuron*, 77(5):969–979.
- 1044 Sigman, M. and Dehaene, S. (2008). Brain mechanisms of serial and parallel processing during  
1045 dual-task performance. *Journal of Neuroscience*, 28(30):7585–7589.
- 1046 Simony, E., Honey, C. J., Chen, J., and Hasson, U. (2016). Uncovering stimulus-locked network  
1047 dynamics during narrative comprehension. *Nature Communications*, 7(12141):1–13.
- 1048 Stark, S. M., Yassa, M. A., and Stark, C. E. L. (2010). Individual differences in spatial pattern  
1049 separation performance associated with healthy aging in humans. *Learning & Memory*, 17(6):284–  
1050 288.

- 1051 Tomrary, A. and Davachi, L. (2017). Consolidation promotes the emergence of representational  
1052 overlap in the hippocampus and medial prefrontal cortex. *Neuron*, 96(1):228–241.
- 1053 Tyng, C. M., Amin, H. U., Saad, M. N. M., and S, M. A. (2017). The influences of emotion on  
1054 learning and memory. *Frontiers in psychology*, 8:1454.
- 1055 Welch, G. B. and Burnett, C. T. (1924). Is primacy a factor in association-formation. *American Journal  
1056 of Psychology*, 35:396–401.
- 1057 Yarkoni, T., Poldrack, R. A., Nichols, T. E., Van Essen, D. C., and Wager, T. D. (2011). Large-scale  
1058 automated synthesis of human functional neuroimaging data. *Nature Methods*, 8(8):665.
- 1059 Yassa, M. A., Lacy, J. W., Stark, S. M., Albert, M. S., Gallagher, M., and Stark, C. E. L. (2011). Pattern  
1060 separation deficits associated with increased hippocampal ca3 and dentate gyrus activity in  
1061 nondemented older adults. *Hippocampus*, 21(9):968–979.
- 1062 Yassa, M. A. and Stark, C. E. L. (2011). Pattern separation in the hippocampus. *Trends In Neuro-  
1063 sciences*, 34(10):515–525.
- 1064 Yonelinas, A. P. (2002). The nature of recollection and familiarity: A review of 30 years of research.  
1065 *Journal of Memory and Language*, 46:441–517.
- 1066 Yonelinas, A. P., Kroll, N. E., Quamme, J. R., Lazzara, M. M., Sauvé, M. J., Widaman, K. F., and  
1067 Knight, R. T. (2002). Effects of extensive temporal lobe damage or mild hypoxia on recollection  
1068 and familiarity. *Nature Neuroscience*, 5(11):1236–41.
- 1069 Zacks, J. M., Speer, N. K., Swallow, K. M., Braver, T. S., and Reynolds, J. R. (2007). Event perception:  
1070 a mind-brain perspective. *Psychological Bulletin*, 133:273–293.
- 1071 Zadbood, A., Chen, J., Leong, Y. C., Norman, K. A., and Hasson, U. (2017). How we transmit  
1072 memories to other brains: Constructing shared neural representations via communication. *Cereb  
1073 Cortex*, 27(10):4988–5000.
- 1074 Zwaan, R. A. and Radvansky, G. A. (1998). Situation models in language comprehension and  
1075 memory. *Psychological Bulletin*, 123(2):162 – 185.

1076 **Supporting information**

1077 Supporting information is available in the online version of the paper.

1078 **Acknowledgements**

1079 We thank Luke Chang, Janice Chen, Chris Honey, Lucy Owen, Emily Whitaker, and Kirsten Ziman  
1080 for feedback and scientific discussions. We also thank Janice Chen, Yuan Chang Leong, Kenneth  
1081 Norman, and Uri Hasson for sharing the data used in our study. Our work was supported in part  
1082 by NSF EPSCoR Award Number 1632738. The content is solely the responsibility of the authors  
1083 and does not necessarily represent the official views of our supporting organizations.

1084 **Author contributions**

1085 Conceptualization: A.C.H. and J.R.M.; Methodology: A.C.H., P.C.F. and J.R.M.; Software: A.C.H.,  
1086 P.C.F. and J.R.M.; Analysis: A.C.H., P.C.F. and J.R.M.; Writing, Reviewing, and Editing: A.C.H.,  
1087 P.C.F. and J.R.M.; Supervision: J.R.M.

1088 **Author information**

1089 The authors declare no competing financial interests. Correspondence and requests for materials  
1090 should be addressed to J.R.M. (jeremy.r.manning@dartmouth.edu).